![UiT The Arctic University of Norway]

Department of Medical Biology, Faculty of Health Sciences

Non-Invasive Methods for Detection of Genetic Abnormalities in Human Embryos

Cell-Free DNA Secreted from Human Embryos as an Alternative to DNA from Cell Biopsies for Genetic Analyses

Viktoria Emeline Swaty Finanger

Master Thesis in Biomedicine, MBI-3911, May 2022

Supervisor: Mona Nystad (Cand Scient, PhD) and Co-Supervisor: Martha Hentemann (MD, PhD)
Women's Health and Perinatology Research Group, Department of Clinical Medicine, Faculty of Health Sciences, UiT - The Arctic University of Norway
IVF-unit, Women's Clinic, Department of Obstetrics and Gynecology, University Hospital of North Norway

Abstract

Chromosomal abnormalities are one of the main causes of implantation failure following embryo transfer in *in vitro* fertilization (IVF). Preimplantation genetic testing for aneuploidies (PGT-A) is time-consuming, expensive, and invasive. Non-invasive PGT-A (niPGT-A) is an alternative where secreted embryonic cell-free DNA (cfDNA) in spent culture medium (SCM) is investigated. This study aimed to investigate and prepare for the implementation of niPGT-A in the IVF-unit at UNN.

To reach this objective 36 anonymized frozen embryos were thawed, cultured and DNA from dissociated cells and SCM was extracted. Furthermore, two different analysis methods were chosen: digital droplet PCR (ddPCR) and Oxford nanopore sequencing. The latter required amplification by Repli-G in advance. ddPCR was performed to investigate genes located on chromosomes 21 (*RUNX1* and *BRWD1*) and 18 (*TCF4* and *SMAD4*), to identify trisomy 21.

The embryos were viable, with DNA present in every sample, having a mean of 1.289 ng/µl throughout the samples. Repli-G was used to amplify five of the embryos, which gave a mean of 2099.29 ng/µl, resulting in over a thousandfold increase in concentration. The amplified samples were then sequenced, which resulted in a blocked run and limited output, with the numbers of reads generated ranging from 7607 to 90 632. Yet, a consensus sequence was generated from the cfDNA found in the SCM sample of embryo 18, which was found to match the human genome. The samples run on ddPCR had a detection of genes involved in trisomy 21, with 11 out of 18 samples having positive droplets generated for the probes targeting the genes located on chromosome 21. The starting concentrations ranged from 0.599 copies/µl to 4.35 copies/µl in the samples with positive droplets detected. There was, however, a lack of detection on the probes targeting the genes located on chromosome 18.

In conclusion, further investigation into both nanopore sequencing and ddPCR is necessary to validate their clinical relevance, however, the possibility of using cfDNA as an alternative to cell biopsies to screen the embryos is promising.

Acknowledgements

Table of Contents

List of Figures

List of Tables

Abbreviations

aCGH	Array comparative genome hybridization
ART	Assisted reproductive technology
BF	Blastocoel fluid
BRWD1	Bromodomain and WD repeat domain containing 1
CCS	Comprehensive chromosome screening
cfDNA	Cell-free DNA
cffDNA	Cell-free fetal DNA
CNV	Copy number variation
ddPCR	Digital droplet PCR
DSB	Double-strand break
DTT	Dithiothreitol
ESHRE	European society of human reproduction and embryology
FISH	Fluorescence *in situ* hybridization
FU	Fluorescence unit
Hg38	Human genome assembly 38
ICM	Inner cell mass
ICSI	Intracytoplasmic sperm injection
IVF	*In vitro* fertilization
MDA	Multiple displacement amplification
MI	Meiosis I
MII	Meiosis II
MPS	Massive parallel sequencing
NGS	Next generation sequencing
niPGT-A	Non-invasive preimplantation genetic testing for aneuploidies
OPU	Ovum pick up

PBS	Phosphate-buffered saline
PGT	Preimplantation genetic testing
PGT-A	Preimplantation genetic testing for aneuploidies
PSSC	Precocious separation of sister chromatids
qPCR	Quantitative PCR
REK	Regional Committee for Medical and Health Research Ethics in Norway
RUNX1	Runt related transcription factor 1
SCM	Spent culture medium
SMAD4	SMAD family member 4
SNP	Single nucleotide polymorphism
TCF4	Transcription factor 4
TE	Trophectoderm
UPD	Uniparental disomy
WGA	Whole-genome amplification

1 Introduction

Assisted reproductive technology (ART) has become a demanding new field in medicine as infertility and the inability to conceive children have increased. It's estimated that 25 million European citizens and one in six couples are affected by infertility of some sort during their reproductive lifetime (1). Infertility has especially become an issue with cultural problems such as obesity, smoking, and alcohol becoming more normalized, along with the environmental pollution decreasing fertility rates (2-4). To aid in the process of conceiving children, *in vitro* fertilization (IVF), a procedure where the oocyte is fertilized with sperm outside the body and then implanted into the woman has become more and more used worldwide (5). Chromosomal abnormalities are one of the main causes of implantation failure, thus, only embryos without chromosomal abnormalities such as aneuploidies are desired for transfer (6-9). However, the identification of viable embryos for transfer represents one of the challenges with ART (10). Another challenge is the method used for embryo testing, which requires experienced and specially trained technicians that can analyze a small number of cells looking for genetic abnormalities. This area of genetic testing is called preimplantation genetic testing (PGT). Currently, preimplantation genetic testing for aneuploidies (PGT-A) is an expensive and invasive method where a biopsy is taken of either the polar bodies, two cells on the 8-cell stage, or of the trophectoderm (TE) of the blastocyst to obtain the genetic status of the embryo (11). Therefore, the development and use of non-invasive PGT-A (niPGT-A) is desirable. One such promising prospect of niPGT-A is using embryonic cell-free DNA (cfDNA) found in the spent culture medium (SCM) that the embryos are cultured in (12). This approach is relatively new but could revolutionize the area of PGT-A, not only by leaving the embryos unmanipulated but also by enabling a more accessible approach to the rather expensive and time-consuming PGT-A analysis.

1.1 Human Embryogenesis

Human embryogenesis refers to the development of the human embryo, which begins at fertilization (13). Fertilization occurs when the spermatozoa have entered the oocyte to form a diploid zygote. After the sperm has entered the oocyte, the completion of the second meiotic division of the oocyte is triggered producing a mature oocyte and its second polar body (14). In the cytoplasm of the oocyte, the sperm enlarges to form the male pronucleus while the tail of the sperm degenerates. During the growth of the female and male pronuclei, their DNA is replicated, creating an ootid with two haploid pronuclei. Once the pronuclei fuse together to

form a diploid collection of the male and female DNA, the ootid becomes a zygote (14). The zygote then continues to divide by mitosis into multiple cells in a process known as cleavage (15).

During cleavage, the mitotic divisions of the cells are reductive, meaning they are unaccompanied with cellular growth, thereby producing increasingly smaller cells for each division (16, 17). As a result, the rather large zona pellucida (a membrane with glycoproteins) can maintain its size when the dividing cells within, termed blastomeres, decrease in size as they increase in number. Most commonly, the divisions during cleavage are divided into the 2, 4-, and 8-cell stages, where the blastomeres are synchronous in their division and, as a result, of similar size. However, during cleavage, the blastomeres divide asynchronous (18), giving rise to the intermediate 3-, 5-, 6-, 7-, and 9-cell stages where the blastomere either belongs to the previous or next synchronous cell-stage (19). In these intermediate stages the blastomeres are of different sizes, until they reach a new synchronous step.

Up until the 8-cell stage, the blastomeres arrange loosely, being undifferentiated and aggregated into a sphere enclosed within the zona pellucida of the oocyte (Figure 1). Between the 8- and 16-cell stages, the blastomeres maximize their contact with each other, by forming a compact ball held together by tight junctions, in a process known as compaction (15). When the blastomeres have divided to the 16-cell stage, they form a morula (18).

As compaction continues, the outer cells lose their individuality as they maximize their cell-to-cell contact, while the inner cell becomes segregated from the outer cell by communicating extensively through gap junctions (15, 18). This results in the cells differentiating into two lineages at the morula stage; the surrounding/outer layer of cells called the trophoblasts (collectively called the trophectoderm, TE) and the inner layer of cells called the embryoblasts (collectively called the inner cell mass, ICM) (15). As the cells continue to divide, blastulation and the formation of the blastocyst ensues. Fluid begins to penetrate through the zona pellucida into the intercellular spaces of the ICM during cavitation, creating the fluid-filled space known as the blastocoele (18). At this stage, the embryo is known as a blastocyst (Figure 1). As the blastocyst cavity fills up, the ICM are pushed to one end of the cavity, creating an embryonic pole (20). In the blastocyst, the two cell lineages that have formed now represents the cells that give rise to the body of the embryo itself (i.e., ICM) and the extraembryonic structures (i.e., TE). In preparation for implantation, a process known as hatching initiates (21), meaning that

the zona pellucida becomes thinner and thinner as the blastocyst expands in size, and is completed once the zona pellucida is shed altogether (8).
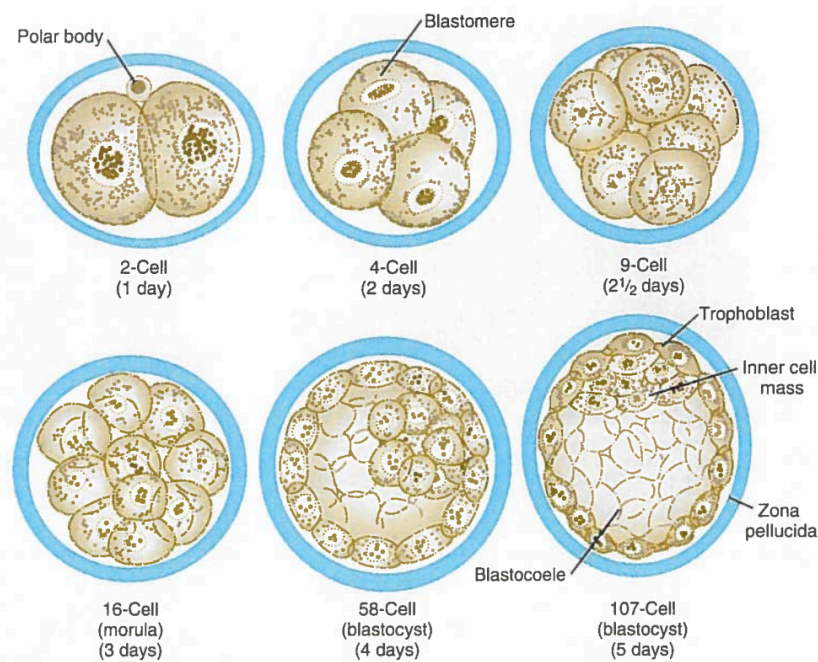
Figure 1 Developmental stages of preimplantation embryos. *The day after fertilization the zygote has split into two cells (blastomeres) with a polar body still present. The blastomeres are enclosed within the zona pellucida (blue). At early day two the blastomeres have had a reductive division; having doubled in number as they decrease in size. At late day two the blastomeres have increased to nine cells and on day 3 they have increased to 16 cells, forming the morula. The zona pellucida starts to expand once fluid starts to penetrate the morula and infiltrate the blastocele cavity. As fluid penetrates the blastomeres, they form two distinct lineages: the trophoectoderm (TE) and the inner cell mass (ICM). Approximately 107 cells are present at day five of embryo development. In the blastocyst at this stage trophoblasts are lining the blastocyst and will eventually form the placenta. The ICM is visible beneath the trophoblast cells immersed in blastocoel fluid. Expansion ensues until the blastocysts starts to hatch, shedding the zona pellucida in preparation for implantation. (18)*

1.2 *In Vitro* Fertilization

Fertilization is as described above, something that naturally happens inside the uterine tubes in the female after an oocyte comes in contact with a spermatozoon (22). However, with IVF, fertilization of the oocyte is performed outside the female body. In 1944 and 1948, the first records of fertilization of human oocytes *in vitro* were published (23, 24), while the subsequent development of human embryos *in vitro* was published in 1955 (25). Robert Edwards then continued the development of IVF and pioneered the reproductive sciences when he successfully implanted a human embryo in 1977, which resulted in the first baby being born from IVF treatment in 1978 (26). Edwards was in 2010 rewarded the Nobel Prize in Medicine for his work (27), and his development has since helped over 8 million babies being born through IVF worldwide (28).

Today, IVF is a modern tool used to combat infertility and help conceiving healthy children by applying different methods to achieve a successful pregnancy resulting in birth of a live-born baby. To perform IVF, mature oocytes and spermatozoa are collected from the female and the male, respectively. Retrieval of the oocytes are often coupled with ovarian stimulation and oocyte maturing injections before retrieval (29), where the oocytes are then collected through a transvaginal ultrasound-guided retrieval (30), called ovum pick up (OPU). The retrieved oocytes can then be fertilized by sperm in a Petri dish containing a special culture medium.

Another approach of fertilizing the oocyte is to inject the sperm directly into the cytoplasm of the oocyte using intracytoplasmic sperm injection (ICSI). It is applied when there is low sperm count and decreased or no sperm motility (31). After successful fertilization by any of the aforementioned methods, the following cleavage of the zygote is monitored microscopically the next days before it is ready to be transferred to the female to, potentially, achieve implantation and pregnancy (14).

1.3 Chromosomal Abnormalities and Aneuploidies

One of the biggest challenges to a successful pregnancy is chromosomal abnormalities in the human preimplantation embryos, causing poor IVF outcome (9). It has been suggested that the majority of chromosomally abnormal embryos are lost either at implantation or shortly after, making most forms of aneuploidy compatible with development to the blastocyst stage (8). To prevent loss of pregnancy after implantation, it is necessary to check the chromosomal status of the embryo before implantation to look for any abnormalities that may affect the implantation and success of pregnancy. Embryos are, therefore, characterized based on their chromosomal profile, which includes aneuploidies, segmental abnormalities, and mosaicism (32).

1.3.1 Aneuploidies

When a diploid cell contains the complete chromosome set of 46 chromosomes it is called euploid, however, whenever a cell deviates from the normal chromosome number of 46 it is called aneuploid (33). Normally, aneuploid cells have an extra chromosome present or a single chromosome absent, resulting in a trisomic or monosomic state, respectively (34). Aneuploidies can also affect numerous chromosomes in a cell, called complex aneuploidy, or result in polysomy or nullisomy where respectively multiple or zero copies of an individual chromosome is present (32).

In preimplantation embryos aneuploidies are primarily a result of meiotic segregation errors (35, 36), meaning errors occurring as the chromosome pairs fail to segregate properly in either the oocyte or sperm and thus affecting all the cells in the resulting embryo (whole-embryo aneuploidy). These segregation errors can be further grouped into non-disjunction errors and premature separation (32). Non-disjunction errors refer to the failure of a pair of chromosomes to segregate properly during one of the two meiotic divisions (Figure 2); either during meiosis I (MI) between homologue chromosomes, or during meiosis II (MII) between sister chromatids. Premature separation, also called precocious separation of sister chromatids (PSSC), occurs when the sister chromatids separate prematurely in MI (Figure 2).
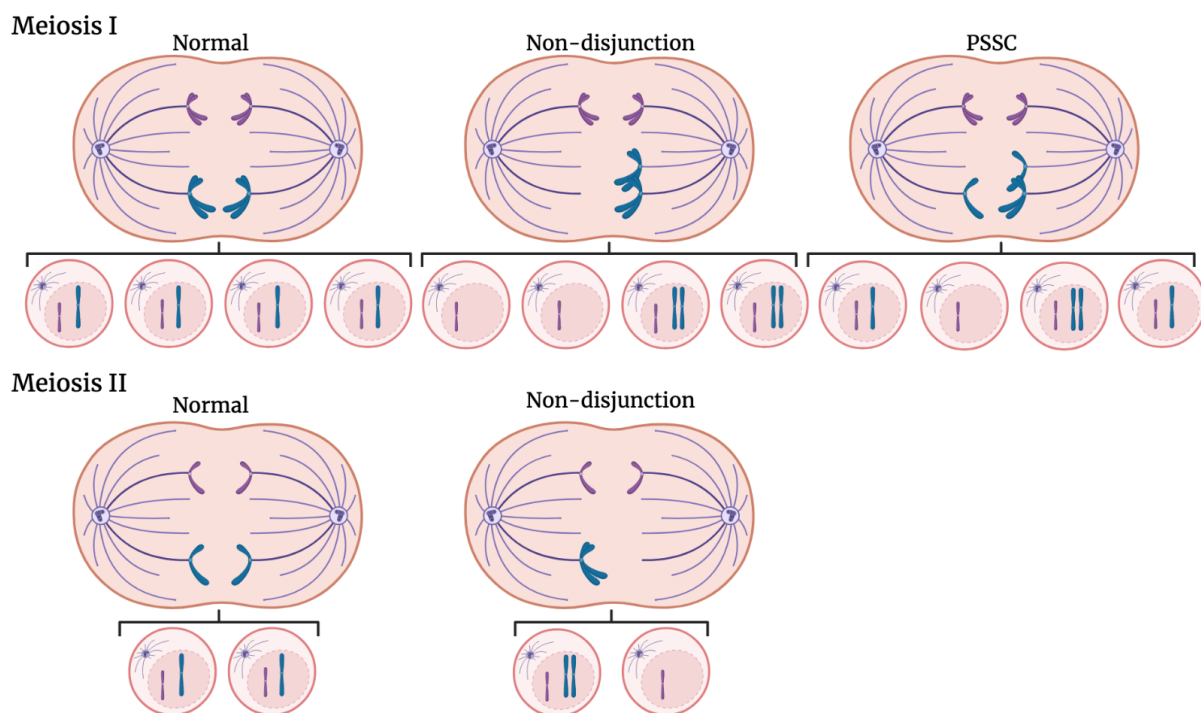
Figure 2 Meiotic segregation errors. *Normal meiosis I (MI) division results in the segregation of homologous chromosomes, where the resulting daughter cells after meiosis II (MII) inherits one copy of each sister chromatid. However, abnormal segregation patterns such as non-disjunction and precocious separation of sister chromatids (PSSC) can occur, where an abnormal number of chromosomes are inherited. Non-disjunction during MI occurs when the homologous chromosomes fail to separate and, therefore, migrate to the same pole, resulting in monosomic and trisomic daughter cells. Non-disjunction during MII occurs when both sister chromatids travel to the same pole, resulting in monosomic and trisomic daughter cells. PSSC occurs during MI where the sister chromatids segregate instead of the homologs, resulting in both normal, monosomic and trisomic daughter cells. Normal MII division results in the segregation of sister chromatids, where each daughter cell have one copy of each chromosome. Figure created using BioRender.*

Several processes in the gametogenesis of oocytes make them more error-prone compared to the spermatozoa (37, 38), resulting in most of the chromosomal aneuploidies originating from the maternal meiosis (37, 39). In males, meiosis is initiated with puberty, and all meiotic events are thereafter sequential. However, in females, meiosis is initiated during fetal development and then arrested in prophase I, where meiosis is not resumed until ovulation in adult life. The

oocyte is then once again arrested in MII, which is only completed if the oocyte is fertilized (40). During the time the oocytes spend in meiotic arrest, the meiotic segregation apparatus seems to gradually degrade causing the chromosome pairs to be erroneously segregated (37, 41). Errors are seemingly more likely to occur during maternal MI than during maternal MII (39, 41, 42), and even less likely to occur during paternal meiotic divisions (32, 39). In addition, a distinctive effect on the ploidy status of the embryo correlated to maternal age has been reported by several studies (43-45). These studies found that the average percentage of euploid embryos was highest for maternal ages of 22 to 28 (~70%), while the percentage decreased after the maternal age of 30 and older (~60%). Reasonably, the percentages of aneuploid embryos were inversed from that of the euploid, having its lowest incidents at the maternal age of 28 (~25%), rapidly increasing after the maternal age of 35, and peaking at the maternal age of 45 (~90%) (44). Furthermore, other studies have found no significant relationship between advanced paternal age and the incidence of aneuploidies in embryos (46, 47).

Even though there are aneuploidies that are compatible with development to the blastocyst stage there are only a few well-defined conditions in which whole-embryo aneuploidies are compatible with survival post-implantation *in vivo* and post-natal life. These conditions include both trisomies of the autosomes; trisomy 21 (Down syndrome), trisomy 18 (Edwards syndrome) and trisomy 13 (Patau syndrome), and of the sex-chromosomes; 47,XXX (Trisomy X), 47,XXY (Klinefelter syndrome) and 47,XYY (Jacob's syndrome) (48). Monosomies of the autosomes and the sex-chromosomes are however, lethal and cannot result in live birth (40, 49), unless they are mosaics as 45,X (Turner Syndrome).

Trisomy 21 is the most common condition caused by aneuploidies found in liveborn (50), and the majority of cases of trisomy 21 are caused by meiotic non-disjunction during MI (~90%) or MII (~10%) (48). The condition has since 1933 been coupled to advanced maternal age (51), where the risk of having an affected child has been found to increase with the maternal age (50). Trisomy 13 and 18 affect multiple systems, are associated with a high risk of fetal death, and are usually fatal within the first few weeks of life (52). Trisomies of the sex-chromosomes are compared to the autosomal trisomies more tolerated and affected individuals often have normal life spans, which makes most trisomies go undiagnosed even though intellect, growth, and speech can be affected (53, 54). Embryos with autosomal trisomies of chromosomes other than 21, 18, and 13 cannot survive post-natal (40), which is why it is important to establish the chromosomal status of the embryo to ensure that the embryo is viable for transfer.

1.3.2 Segmental Abnormalities

Segmental abnormalities affect sub-chromosomal sections and typically denote a genetic imbalance caused by the gain or loss of chromosome material (55). These aberrations originate from erroneous corrections of DNA double-strand breaks (DSBs) (32), which can be induced by various exogenous and endogenous sources (56, 57). They can also be induced by the collapse or stalling of the replication fork, insufficient materials needed for DNA synthesis, and replication challenges associated with secondary structures (56, 57). If these DSBs are not resolved, they can result in the duplication or deletion of the segment that contains the break (Figure 3), creating segmental abnormalities (32). Such aberrations are collectively called copy number variations (CNVs), which range in size from 1Kb up to the Mb-scale (58).
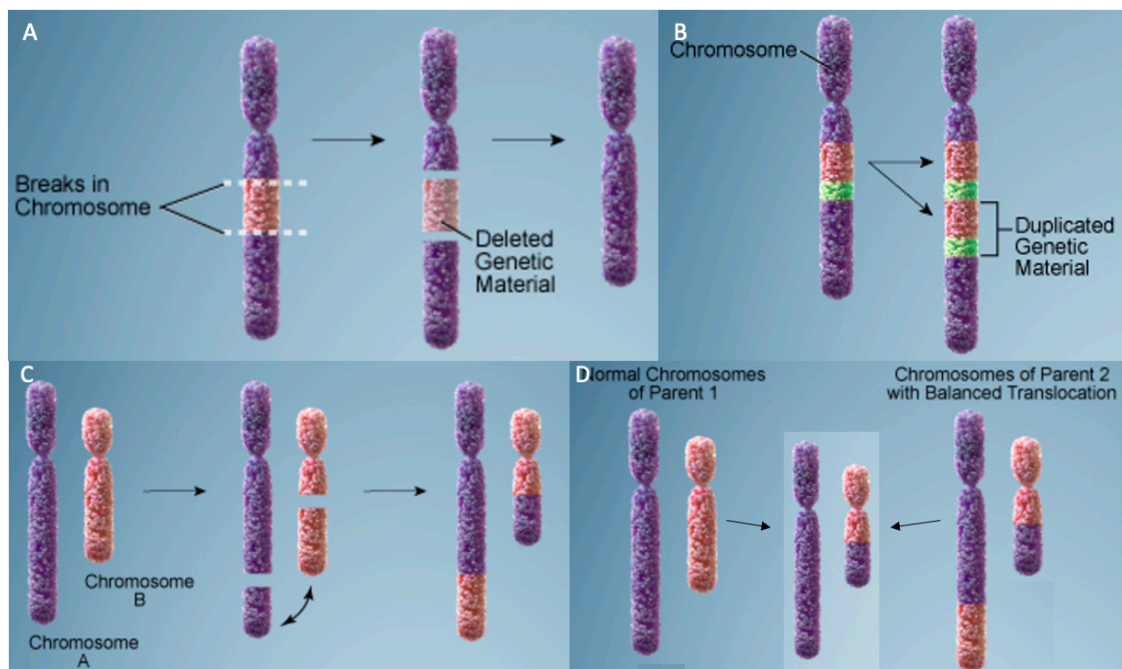
Figure 3 Changes in chromosome structure causing segmental abnormalities. *A) Deletion of a segment causes loss of genetic material. B) Duplication of a segment causes gain of genetic material. C) A reciprocal translocation, of segments between two chromosomes causes a balanced translocation to occur in its carrier. Therefore, there is no gain or loss of genetic material. D) An unbalanced translocation occurs when there is loss or gain of genetic material. This can occur when an offspring of a carrier with a balanced translocation inherits one chromosome from each parent, resulting in an unbalanced chromosome being inherited. Modified from (59).*

A segmental aneuploidy may be created from an error occurring during gametogenesis (60), or be inherited from a parent carrying a balanced translocation where the carrier is phenotypically normal but their gametes carry an unbalanced chromosome (61) (Figure 3). Depending on whether the segmental abnormality was inherited from a parental gamete or created during one of the mitotic divisions, the segmental aneuploidy will either be present uniformly in all cells of the embryo or be present in a mosaic pattern (55, 62). Recent studies have found that the majority of instances of segmental aneuploidy in embryos are from errors of mitotic origin,

making them not only present in a mosaic pattern (60, 63), but also independent of maternal age (64, 65). This is a strong contrast to whole-chromosome aneuploidies, which have been found to have an association with advanced maternal age, suggesting that the molecular processes that causes segmental aneuploidies are different from those responsible for whole-chromosome aneuploidies (56, 66).

The breakage and subsequent repair of a DNA-segment can cause genetic imbalances called segmental abnormalities, which are genetic imbalances, but they can also result in an abnormal combination of segments (i.e. structural chromosome abnormalities) (34). These are not included in the definition of segmental abnormalities as they change the natural order of the chromosome segments, leaving the copy numbers unaltered (32), but are relevant in the terms of embryo-quality. Structural chromosome abnormalities are further divided into balanced and unbalanced rearrangements. Unbalanced rearrangements are generally caused by duplications or deletions, or both, and are as the term implies a result of gain or loss of genetic material causing an imbalance in its carrier. Balanced rearrangements, however, are mostly caused by translocations or inversions, where the embryo of affected individuals is at risk if they inherit chromosomes that become unbalanced during recombination or sorting at meiosis (67). Thus, embryos are directly affected by unbalanced chromosomes, whereas a balanced chromosome pose a threat to the subsequent generation of embryos created by its carrier.

1.3.3 Mosaicism

Aneuploidies can be uniformly present in the embryo affecting all cells as a result of an error occurring meiotically in either the paternal or maternal gametogenesis, as described above, or aneuploidies can be created during any of the mitotic divisions of the preimplantation embryo after fertilization, creating mosaic aneuploidy (32, 68). Embryonic mosaicism is, therefore, when there are two (or more) genetically distinct cell lineages in a single embryo (69). These mitotic errors can occur in the first cleavage process, but has also been found to occur more commonly in the second or third cleavage stage (70).

Mosaicism arises from mitotic errors where sister chromatids fail to segregate properly, such as: anaphase lag, non-disjunction, endoreplication, and centrosome dysregulation affecting the chromatid segregation (32). Anaphase lag results in one normal and one monosomic daughter cell, non-disjunction results in reciprocal monosomic and trisomic daughter cells, while endoreplication causes an excessive replication of a chromosome resulting in a trisomic state of that chromosome in one of the daughter cells (71). The first mitotic divisions are dependent

on the paternally inherited centrosome, which is the active center of division (72). Disruption or dysregulation of this division center could, therefore, result in mosaicism in preimplantation embryos as the chromosomes fail to segregate (73). Research have also found that in cases with severe male infertility the formation of aster is delayed (74, 75), this formation is essential in the male and female pronuclear migration during fertilization and in the embryonic cleavage stages, and could, thus, produce mosaicism in the embryos that are affected (71).

Additionally, there are mitotic events that results in mosaicism while still having a diploid cell line. Uniparental disomy (UPD) is when a cell inherits both copies of a chromosome from the same parent, instead of inheriting one copy from each parent (48). The UPD-affected daughter cell can either be isodisomic by inheriting two identical sister chromatids from one parent, or heterodisomic by inheriting both homologous chromosomes from one parent. Trisomic rescue is the most common cause of UPD (76), which is a mechanisms that is applied by the cell to reinstate a diploid state during mitosis by losing one copy of a duplicated chromosome arising from a mitotic error (48).

Mosaic embryos may be divided into aneuploid mosaic; where there are two different aneuploid populations of cells present, resulting in 100% of the cells within the embryo being abnormal, and diploid-aneuploid mosaic; where there is one diploid and one aneuploid population of cells (77). Additionally, chaotic mosaicism is when a severe pattern of irregularity is shown, where multiple chromosomes are affected and the cells seem to possess a random set of chromosomes (68). The percentage of abnormal cells in a diploid-aneuploid mosaic embryo is affected by which cleavage stage the mitotic error occurs in, as errors occurring at the second cleavage result in a greater portion of abnormal cells compared to errors occurring at the third cleavage (70). However, how the mosaicism influences the implantation and the following development of the embryo, depends on what chromosome is involved in the abnormal genotype and the degree of mosaicism, in addition to what cell lineage is affected by the mosaicism (71).

When the embryo has reached the blastocyst stage, the mosaicism can be further defined according to what cell lineage, either the ICM or the TE, is affected by the aneuploid cells (Figure 4). When all the cells of the ICM are diploid and all those of the TE are aneuploid (or vice versa), an ICM/TE mosaicism is found. Additionally, if the mosaic population is confined exclusively to either the ICM or TE lineage, an ICM mosaicism or TE mosaicism is found. Lastly, a total mosaic embryo is found when aneuploid and euploid cells are distributed indistinctively in both the ICM and TE (11).

Figure 4 Distribution of aneuploid cells in mosaic blastocysts. *ICM/TE mosaic embryos are found when the aneuploid cell lineage is confined to either the ICM or the TE. TE mosaic embryos are found when the aneuploid cells are found exclusively in the TE, and ICM mosaic embryos are found when the aneuploid cells are found exclusively in the ICM. Total mosaic embryos are found when the aneuploid cells are indistinctly distributed in both cell lineages. ICM; Inner cell mass, TE; Trophectoderm. Modified from (11).*

1.4 Morphological Assessment

In addition to characterizing the embryos based on their chromosomal profile, they are also assessed based on morphological features, which is essential in selecting the embryos with the highest development potential (78). Embryos are during the different stages of development; cleavage stage (day 2 and day 3), morula stage (day 4), and blastocyst stage (day 5) assessed according to the Istanbul criteria (79). During the cleavage stage, the embryos are given a score based on features such as the number of blastomeres, their size and symmetry, and fragmentation and multinucleation (Appendix A). During the morula stage, the embryos are given a score based on what stage of cleavage they are in and their compaction development (Appendix B). Finally, during the blastocyst stage, the embryos are given a score based on their developmental and expansion stage, as well as the quality of their ICM and TE (Appendix C). These scores do not just indicate whether an embryo is fit for transfer, but they also determine whether their morphology is compatible with genetic screening and cryopreservation, or not, during the entire preimplantation development (80).

This new consensus grading system was developed so that the same criteria for morphological assessment of embryos could be applied to all IVF-laboratories practices globally (79). It was developed by already existing grading schemes such as the widely used scoring system introduced by Gardner and Schoolcraft in 1999 (81), however, it has one important change, the introduction of numerical scores. Previously the embryos had been given a letter grade that represented their quality, where A was best, and D was worst. Now, instead a number from 1

to 3 is given for the cleavage and morula stage, as well as the quality of the ICM and TE, and a score of 1 to 4 is given on the stage of development of the blastocysts. This change enables mathematical computations to be made of the embryo quality, and as a result, allows inter-clinical comparisons to take place (79). Having a common terminology and a standardized practice of minimum criteria used to grade embryos, creates a safe and effective treatment of IVF patients, alongside driving the development of products and better technologies forward, as the discrepancies of embryo quality and viability is easier to detect and potentially solve.

1.5 Genetic Testing of Embryos

As aneuploidies and other chromosomal abnormalities in the embryos are one of the biggest challenges to couples undergoing IVF treatment, PGT-A was implemented into IVF programs to aid in the improvement of pregnancy rates and decrease miscarriage rates (11). The molecular strategies applied for PGT-A have improved over the years as technical progressions have been made in molecular genetics, as well as in culture systems and cryopreservation protocols, allowing more reliable results from genetic testing to be produced (82). Initially, fluorescence *in situ* hybridization (FISH) was used in PGT-A, but one limitation to this approach is that FISH is only applicable to analyze a limited number of chromosomes. Yet, with better technologies emerging, the analysis of the 23 chromosome pairs was possible with methods such as quantitative PCR (qPCR), array comparative genome hybridization (aCGH), single nucleotide polymorphism (SNP) arrays, and next generation sequencing (NGS). In recent years PGT-A has been further developed to reduce its invasiveness, and a new area of PGT-A was born; niPGT-A. This approach is still under development and has yet to be implemented clinically but is a promising new aspect of genetic testing of embryos.

1.5.1 Evolution of the Biopsy Strategy

Embryo biopsy is an essential step in the PGT-A of embryos and have evolved over the years to accommodate biological criteria and technical criteria. Originally, a biopsy was performed on cleavage-stage embryos by removing one or two blastomeres from an 8-cell embryo (Figure 5;a), however, with advancements in culturing systems and the poor understanding of commitment of cell lineage in cleavage-stage embryos, embryo biopsy on the blastocyst stage has been possible and is now favored biopsy strategy
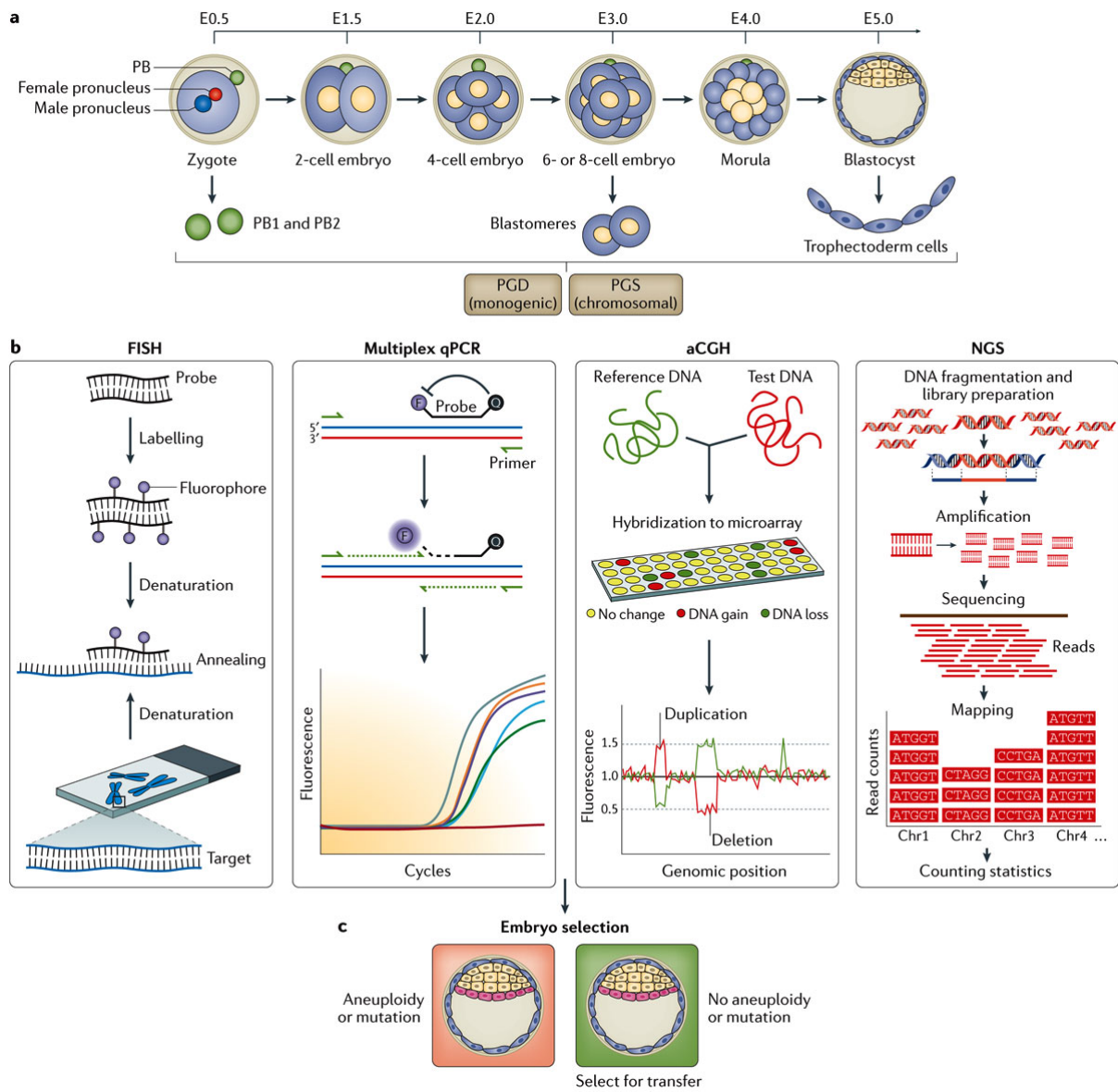
Figure 5 Preimplantation diagnosis and screening (PGD/PGS). *a) The embryonic development stages (e.g., day 3.0 (E3.0)) of an in vitro fertilization (IVF) derivative embryo and the cells used for biopsy to perform preimplantation genetic testing of aneuploidies (PGT-A). The biopsies can be taken as polar bodies (PB), blastomere(s) or from the trophoectoderm (TE) wall. b) The methods applied in PGT-A are fluorescence in situ hybridization (FISH), multiplex quantitative PCR (qPCR), array comparative genomic hybridization (aCGH) and low coverage next generation sequencing (NGS). c) Embryos are selected for transfer based on their chromosomal content, where embryos without any detected aneuploidies are selected. Chr; Chromosome, F; Fluorophore, Q; Quencher. (83)*

Biopsies taken from the TE wall of the blastocyst removes a smaller portion of the embryonic biomass compared to a cleavage-stage biopsy, in addition to only obtaining cells already committed to the extra-embryonic lineage (82). These inherent advantages of blastocyst biopsy, combined with the emergence of comprehensive chromosome screening (CCS) where the entire chromosome complement is assessed, resulted in the development of better diagnostic strategies (84). The higher number of cells collected provides a greater amount of DNA for downstream analysis and, therefore, a more reliable test result, reducing the risk of false positives and false negatives and increasing technical reproducibility and diagnostic rates (82).

Collectively this have resulted in an improved strategy for investigating the genetic composition of embryos involved in IVF treatment.

1.5.2 Evolution of PGT-A Methods

The first method to be introduced in the diagnostic strategy of detecting aneuploidies in embryos was FISH-analysis, which involves fixation of the blastomere biopsied on a glass slide and the subsequent hybridization of chromosome-specific fluorescent DNA probes (Figure 5;b). Fluorescent microscopy is then applied to detect the absence or presence of the specific DNA sequence that the probes were targeted against, and the results are provided within 2-3 days (85). Previously FISH has been the most applied method of aneuploidy screening, but its utilization has declined globally (86), due to its limitation in the number of chromosomes analyzed and with publications finding high incidences of false positive results associated with mosaicism and single-cell analysis (87-89).

Instead, more reliable CCS technologies, such as qPCR, SNP array, and aCGH, have been applied (Figure 5;b). These technologies are all able to accurately assess all 24 chromosomes, allow parallel sample analysis, and can, therefore, provide more reliable results and a higher throughput than FISH (82). Analysis by qPCR usually requires 4 probes per chromosome to analyze all 24 chromosomes and was developed as a faster and cheaper alternative to the array platforms, taking only 4 hours to complete analysis (90). A large study conducted on the comparison of aCGH and qPCR found high concordance between them when the standard criteria for diagnosis of whole chromosome aneuploidies were used (91), the downfall of these methods are, however, their inability to detect mosaicism (92).

Another new CCS technology that also allows parallel sample analysis and provides a high throughput, is NGS (Figure 5;b). NGS systems are not only sensitive and provide reliable results of whole chromosome aneuploidy, but they also provide higher accuracy in the assessment of segmental aneuploidies and can also detect low-level mosaicism with accurate discrimination of the proportion of cells showing the abnormal karyotype (93). Analysis of the biopsied DNA is dependent on whole-genome amplification (WGA) to provide a sufficient amount of DNA for the subsequent library constructions, where the generated products are fragmented into smaller fragments, which then are sequenced in parallel (94). The sequences are called "reads" and are aligned to a human reference genome, where the relative number of reads that map onto each chromosome indicates the chromosomal status of the embryo

analyzed; where an increase indicates an additional chromosome present, while a decrease indicates the absence of a chromosome.

The latest technology that has emerged in the genetic testing of embryos is Nanopore sequencing (Figure 6). This type of sequencing uses voltage change across nanopores fixed in a flow-cell membrane, making the technique entirely different from NGS. Nanopore sequencing provides some advantages over the other CCS methods, not only has it been shown to have sensitivity equal to NGS in detecting whole chromosome abnormalities (95), but it is also considerably cheaper, and only uses ~2 hours for overall analysis allowing the analysis to take place in the IVF laboratories (82).
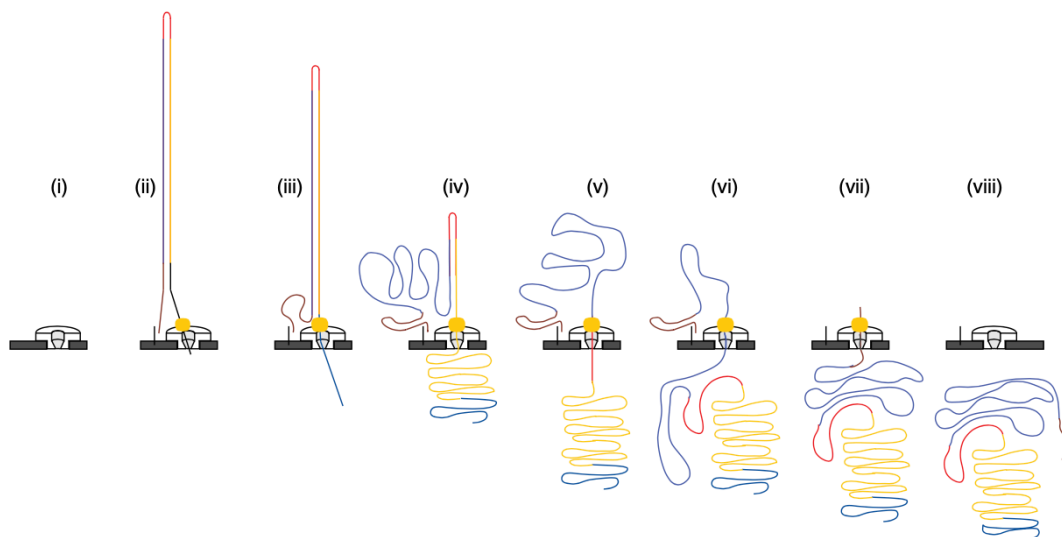
Figure 6 The steps of sequencing DNA through a Nanopore. i) The nanopore channel open. ii) A dsDNA molecule with the adaptors; lead adaptor (blue), bound molecular motor (orange), hairpin adaptor (red) and trailing adaptor (brown) ligated, and being captured by the nanopore. Following capture is the passing of the iii) lead adaptor, iv) template strand (gold), v) hairpin adaptor, vi) complement strand (dark blue) and vii) trailing adaptor through the nanopore. viii) The nanopore channel then returns to open. (96)

1.5.3 Non-Invasive Alternative to Genetic Testing

With the advancing technologies in the molecular genetics field, new approaches to genetic testing, which are non-invasive to the embryo have been proposed. This area of preimplantation genetic testing is called niPGT-A and is based on the presence of embryonic cfDNA in both the blastocoel fluid (BF) of the blastocyst (97) and the SCM that the embryos are cultured in (12, 98). Aspiration of the BF is performed through a technique called blastocentesis (99), which is somewhat invasive to the embryo as it punctures the zona pellucida, but since it does not remove any biomass it is still considered minimally invasive. Aspiration of the SCM is, however, totally non-invasive as the embryo is not manipulated in any way, allowing the chromosomal composition of the embryo to be analyzed without removing any biomass (Figure 7).

Several studies have analyzed cfDNA found in the SCM and compared these to the biopsies of the TE (98, 100-103) and to biopsies of the whole blastocyst (104), where the concordance rates were increased when biopsies of whole blastocysts were used. This suggests that using niPGT-A with cfDNA could give a more reliable representation of the chromosomal status of the embryo than conventional PGT-A using TE biopsies can (104). Nonetheless, the origin of embryonic cfDNA is yet unknown, and further research is necessary to fully address its representativeness of the embryo and its use in the IVF clinics.
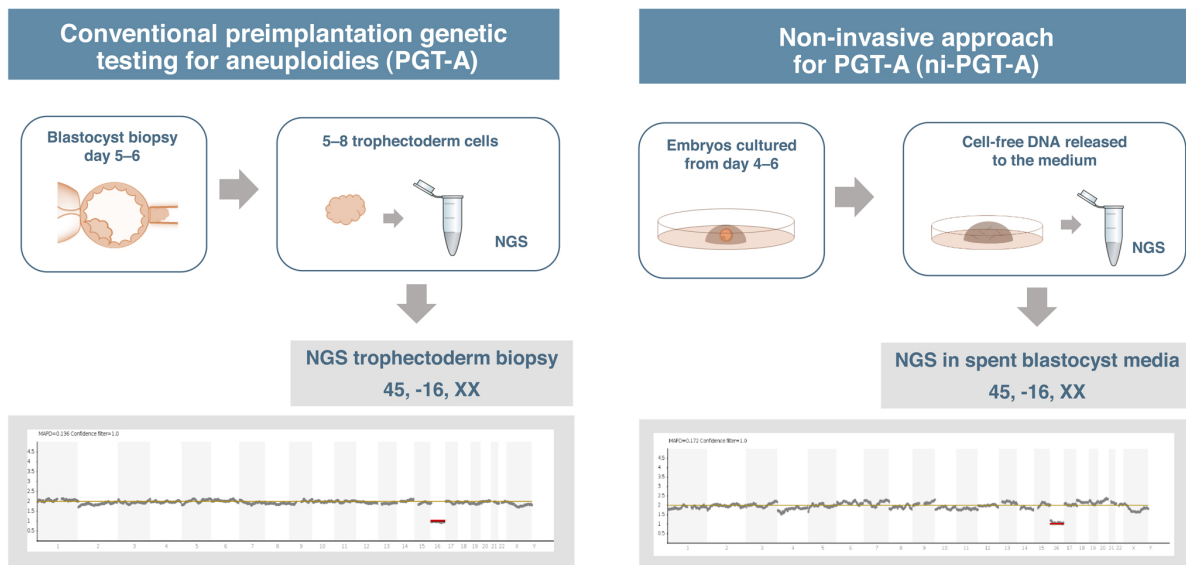
Figure 7 Comparison of the conventional cell biopsy and the non-invasive approach for preimplantation genetic testing for aneuploidies (PGT-A). In conventional PGT-A, an invasive biopsy of the cell in the trophoectoderm (TE) wall is removed for analysis, while in non-invasive PGT-A (niPGT-A), the spent culture media (SCM) that the embryos are cultured in are collected for analysis of embryonic cell-free DNA (cfDNA). NGS; Next generation sequencing. (11)

2 Aim and Objectives

The overall aim of this Master's thesis was to optimize the sampling preparation steps of the human embryo to prepare for implementation of PGT-A in the IVF clinic at UNN, using embryo-culturing, phase contrast microscopy, invasive- and non-invasive biopsy sampling, and targeted gene analysis as well as whole genomic methods for aneuploidy analysis of embryos.

The specific objectives were:

- To optimize the sampling steps for different embryo biopsies, i.e., spent culture medium and whole blastocyst biopsies.
- To evaluate different media to get good downstream aneuploidy results of spent culture medium biopsies.
- To investigate suitable methods for genome amplification.

- To implement investigation of embryonic cell-free DNA by digital droplet PCR and Nanopore sequencing.

3 Material and Methods

All embryos used in this study were from anonymous donors from the IVF-unit's old biobank. Informed consent was taken from each couple donating and the Regional Committee for Medical and Health Research Ethics in Northern Norway (REK) approved the use of these embryos (REK-approval #2017/1085 Nanoscopic Study of Human Embryos). To learn the skills and techniques required to culture and handle the embryos, the first few weeks in the laboratory were used to thaw and culture embryos from different cleavage stages (day 3) and blastocyst stages (day 5). During these weeks the embryos were cultured in old media, which the embryos responded positively to by continuous development. Morphological assessment was also performed in these weeks, to learn what characterizes the embryos during the different stages of development. Both picture-perfect embryos were visualized during these weeks, in addition to heavily fragmented ones. The embryos cultured during the same weeks were used to test if any cfDNA could be identified in the SCM and were used in initial runs of digital droplet PCR (ddPCR). After learning the techniques and skills necessary to handle the embryos, the embryos cultured from there on out were treated with the appropriate new culture media to properly illustrate the full capacity of embryo culturing and its application in downstream analysis and testing.

3.1 Embryo Thawing

All embryos used in this study were cryopreserved after their donation and stored in liquid nitrogen, so to isolate DNA from the embryos and their SCM, they were first thawed. Embryos were either cryopreserved on day 3 or day 5 during their original use in the IVF clinic and based on their developmental stage they were thawed in different media containing the right nutrients necessary for their development. Embryos in the cleavage stage have low biosynthetic activity and does, therefore, require less additives in their media compared to embryos post-cleavage, which have high biosynthetic activity (105). However, the companies producing these do not disclose the exact reagents in their media and what each media specifically contains is consequently unknown.

Before the embryos were thawed, 300 µl of the thawing media and culturing media were pipetted onto a 5-well culture dish and pre-warmed for a minimum of 2 hours in the incubator

set to 37°C and 5% CO_2 before use. The straws containing the embryos were retrieved from the liquid nitrogen tank and placed on the lab bench for 30 seconds, followed by 1 minute in 30°C sterilized water to melt. The embryos were then removed from the straw by cutting one end off and attaching the open end to a silicon tube connected to a 1ml syringe filled with air, the other end was then cut off and the embryo was slowly pushed out from the straw and into the thawing media. Transfer of the embryo was performed under the phase microscope to detect the position of the embryo more easily in the media.

Embryos cryopreserved on day 3, had four thawing media (Embryo Thawing Pack), where the embryos were incubated in thawing media 1 and 2 for 5 minutes at room temperature, thawing media 3 for 10 minutes at room temperature and were only in thawing media 4 for a quick rinse before immediate transfer to the incubation media. Embryos cryopreserved on day 5 on the other hand only had two thawing media (BlastThaw) and were incubated in thawing media 1 and 2 for 10 minutes at room temperature before their transfer to the incubation media. A sterilized handling pipette (127-129 µm) was used to transfer the embryos between the different thawing media. Each embryo was handled with their own sterilized pipette to avoid contamination of the thawing media or culturing media with DNA-residues or other contaminants from other embryos.

Once the embryos had thawed and had been transferred to their incubation media, the 5-well culture dish containing the embryos were placed back in the incubator for further development. The reagents needed to thaw and culture the embryos are listed in Table 1 and the equipment are listed in Table 2.

Table 1 Reagents used to thaw embryos frozen on day 3 or day 5 and to culture them.

Reagents	Manufacturer	Catalog Number	Lot number	Country
Embryo Thawing Pack	Origio	10430010A	17070062	Denmark
BlastThaw	Origio	1054210A	21270039	Denmark
Quinn's Advantage Cleavage Medium	SAGE	ART-1026	21325016	UK
Quinn's Advantage Blastocyst Medium	SAGE	ART-1029	17290070	UK

Equipment	Manufacturer	Catalog Number	Lot number	Country
HyPure™ Molecular Biology Grade Water	Cytiva	SH30538.02	AG29749941	USA

Table 2 Overview of equipment used to thaw frozen embryos.

Equipment	Manufacturer	Catalog Number	Lot number	Country
5-well culture dish	Vitrolife	16004	11780, 12059	Sweden
15ml SuperClear Centrifuge Tubes	VWR	93000-022	4122-440CE-440C	USA
BioClean Ultra™ 1000µl RT LTS Pipette Tips	Mettler Toledo	30389212	20722	USA
Rainin Classic Pipette PR-1000	Rainin	17008653	LO938944A	USA
Handling Pipette 127-129 µm	Vitrolife	15531	2111002, 2111023	Sweden
Grip for Handling Pipette	Vitrolife	15458	2111026	Sweden
Rack for Handling pipette	Vitrolife	15459	2111037	Sweden
Sterile Luer Slip 1ml Syringe Without Needle	BD Plastipak	303172	210615	USA
Silicone Tubing, 4x7 mm	VWR	228-1452	3218283	USA
CO_2 water jacketed incubator	Forma Scientific	S/N 26586-446	-	USA
Thermolyne Locator Jr. Cryo Storage	Barnstedt Thermolyne Corp.	38-3282-9	-	USA

3.2 Embryo Culturing

The media used as the last step in the thawing process, the incubation media (Table 1), is the same media that the embryos were cultured in. Each embryo was cultured in a separate dish in

order to collect the embryonic cfDNA secreted out into the media and to perform downstream analysis.

During the embryonic development, the culture media was only changed for day 3 embryos. Once the embryos reached the morula stage, they were placed in the culturing media for blastocysts to encourage further development. Before transfer, 300 µl of the blastocyst culturing media was pre-warmed in the incubator at 37°C and 5% CO_2 for at least 2 hours. Transfer of the embryos were then performed using a handling pipette (127-129 µm) under the phase microscope, where the old media was collected and stored at -20°C for later DNA purification and downstream analysis.

3.2.1 Morphological Assessment

After the embryos have been cryopreserved, they are often shrunken and needs time to expand to their true size. Morphological assessment of the embryos was, therefore, performed 1 hour after thawing for day 3 embryos and 4 hours after thawing for day 5 embryos. During the culturing of the embryos in the following days, they were assessed at the same time-point each day every day, to record their development every 24 hours. Morphological assessment was performed using the equipment listed in Table 3, with pictures taken to document their development.

Table 3 Equipment used for microscopy and to take pictures of the embryos.

Equipment	Manufacturer	Catalog Number	Lot number	Country
Eclipse Ts2 E50L50 Inverted Microscope	Nikon	M700EN08	-	Japan
DeltaPix HDMI 16MDPX camera	DeltaPix	DO3621142	-	Denmark
Hp E24i G4 WUXGA screen	Hp Inc.	HSD-0056-9	-	USA

3.3 Embryo Sampling

Once the embryos had reached the blastocyst stage and expanded sufficiently, samples from either the SCM or of the whole blastocyst was taken. The embryos were originally intended to have multiple biopsies performed (including from the TE, ICM and BF) to have a greater

comparison and, thus, get a better understanding of the different biopsy's representation of the genetic composition of the embryo. However, due to lack of time, equipment, and training to perform these biopsies, only SCM and whole blastocyst biopsies were performed. The different entry points for sampling were given a number to represent what type of biopsy that was performed before the lab-work started, which is why SCM is represented by x.1, and whole blastocyst dissociation biopsy is represented by x.5.

Samples from the SCM were taken by removing the embryo from the incubation media using a handling pipette (127-129 μm) and placing the embryo in another dish containing fresh media for subsequent biopsy taking. Once the embryo had been removed from the SCM, the SCM was collected and prepared for storage. The embryos that were thawed at day 5 had no change in culture media and their SCM was, therefore, collected into a new sterile Eppendorf tube. The embryos that were thawed at day 3 did, however, have a change in culture media, and their SCM was, therefore, collected into the same Eppendorf tube as their old SCM.

Samples taken of the whole blastocyst was taken by first removing the embryo from the original SCM and then placing it in a drop of 20 μl of fresh blastocyst incubation media in a Centre well dish. The embryo was then mechanically dissociated by repeated resuspension in the media using a handling pipette (134-145 μm). This was performed under the microscope, allowing the cells to be observed during the dissociation, where the number of resuspensions could be adjusted according to the needs of each embryo. Once the embryo had dissociated, the TE cells were undistinguishable from the ICM cells, and the entire sample was collected and prepared for storage.

Once the samples had been collected from the SCM or the whole blastocyst, the samples were stored at -20°C until further analysis was performed. The equipment needed to take the different type of biopsies from the embryos are listed in Table 4 and the reagents are listed in Table 1.

Table 4 Equipment used to take biopsies from the embryos.

Equipment	Manufacturer	Catalog Number	Lot number	Country
BioSphere® SafeSeal Tube 1.5 ml	Sarstedt	72.706.200	0081421	Germany
Centre well dish	Vitrolife	16005	M343420	Sweden

Handling Pipette 134-145 µm	Vitrolife	15533	2111009	Sweden
BioClean Ultra™ 20 µl RT LTS Pipette Tips	Mettler Toledo	30389225	30729	USA
BioClean Ultra™ 1000 µl RT LTS Pipette Tips	Mettler Toledo	30389212	20722	USA
Rainin Classis Pipette PR-10	Rainin	17008649	D1080682A	USA
Rainin Classic Pipette PR-1000	Rainin	17008653	LO938944A	USA

3.4 Extraction and Purification of DNA

To analyze the genetic composition of the embryos, the DNA needs to be extracted from the embryonic cells and purified from the culture media to remove any contaminants before further downstream analysis is performed.

The embryonic cfDNA from the SCM and the embryonic DNA from the whole blastocyst biopsy samples were purified using the QIAamp® MinElute Media Kit from Qiagen according to the manufacturer's instruction, except the vacuum system was replaced with a conventional centrifugation system. The kit uses the well-established QIAamp technology for the purification of nucleic acids, where the selective binding properties of the nucleic acids to the silica-membrane is utilized. It is well suited for liquid samples, such as the SCM containing cfDNA, where the purified nucleic acids from the sample are washed to remove any contaminant such as proteins, nucleases, and other impurities before they are eluted into the AVE-buffer for further downstream analysis or storage between -30°C to -15°C.

The input volume from the stored frozen samples were 300 µl or 600 µl for the SCM samples (as day 4 embryos had their culture media changed and, therefore, double the volume), and 20 µl for the cell-biopsies. The lysate (i.e., sample together with reagents) was run through the column in two intervals of 500 µl, to compensate for the lager input volume of the SCM samples. During the washing steps, the columns were centrifuged at 8000 rpm (6000 g) for 1 min instead of applying the vacuum system. Each sample had their purified DNA eluted in 20 µl AVE-buffer, except for both samples from embryos 8-19 which had their DNA eluted in 120

µl AVE-buffer. The equipment needed to purify the cfDNA from the SCM samples and the DNA from the whole blastocyst biopsies are listed in Table 5 and the reagents are listed in Table 6.

Table 5 Equipment needed to extract and purify the DNA from the embryo biopsies.

Equipment	Manufacturer	Catalog Number	Lot number	Country
QIAamp® MinElute Media Kit	Qiagen	57414	169044764, 169049481	Germany
QIAamp® MinElute Column	Qiagen	1020909	1690375743,	Germany
15ml SuperClear Centrifuge Tubes	VWR	93000-022	4122-440CE-440C	USA
DNA LoBind Tubes 2 ml	Eppendorf	022431048	D1555051	Germany
BioClean Ultra™ 200 µl RT LTS Pipette Tips	Mettler Toledo	30389239	61042	USA
BioClean Ultra™ 1000 µl RT LTS Pipette Tips	Mettler Toledo	30389212	20722	USA
Rainin Classic Pipette PR-100	Rainin	17008651	LO93727A	USA
Rainin Classic Pipette PR-1000	Rainin	17008653	LO938993A	USA
Reax top vortex	VWR	444-0098	-	USA
Mini Star Silverline	VWR	3700-930	-	USA
ThermoMixer C	Eppendorf	5382000015	-	Germany
Biofuge 13	Heraeus	3645	-	Germany
IEC Centra-M centrifuge	IEC	05862	-	USA

Table 6 Reagents needed to purify the DNA from the embryo biopsies.

Reagents	Manufacturer	Catalog Number	Lot number	Country
Ethanol absolute	VWR	20821.296	20F104008	USA
AVE-Buffer	Qiagen	57414	169038753, 169045357	Germany
AL-Buffer	Qiagen	574145	169040971, 169041001	Germany
ATL-Buffer	Qiagen	57414	169038720, 169038720	Germany
AW2-Buffer	Qiagen	57414	169041562, 169044465	Germany
Carrier RNA	Qiagen	57414	169037603, 56902183	Germany
Proteinase K	Qiagen	57414	169027684, 169047082	Germany

3.4.1 Correcting the Wrong Elution Volume

Both samples from embryos 8-19 had their isolated DNA eluted into 120 µl instead of 20 µl, making their already low DNA concentrations 5 times more diluted compared to the rest. To correct this mistake, these samples were concentrated by a Genevac miVac centrifuge set to 43°C for 90 minutes to remove the water and other solvents in the AVE-buffer by evaporation, thus, only leaving the isolated nucleic acids in a pellet. The pellets of nucleic acids could then be resuspended in the correct volume of 20 µl of the AVE-buffer, leaving them with the same elution-volume as the rest of the samples and the right dilution factor. The equipment needed to concentrate the samples is listed in Table 7, and the reagent is listed in Table 6.

Table 7 Equipment needed to concentrate the samples with a higher elution volume.

Equipment	Manufacturer	Catalog Number	Lot number	Country
Genevac miVac Centrifugal Concentrator	Thermo Fisher Scientific	12080192	-	USA

3.5 Measuring DNA Concentration

Hands-on quantitation was performed by the lab manager at the genomic support center at UiT, due to restrictions in work regulations.

There is around 6 pg DNA per eukaryotic cell (32), making the amount of DNA present in the different samples remarkably low, even when the whole blastocyst, containing between 64 and 256 cells (106), is analyzed. Conventional molecular analysis requires more DNA, making it necessary to quantitate the amount of DNA present in each sample, so that they can be applied to the right downstream analysis. For this study, Qubit and NanoDrop was used to find the most reliable quantitation method.

3.5.1 Qubit

The Qubit Quantitation Platform uses fluorescent dyes to detect and measure the concentration of the specific molecules of interest, in this case DNA, and is able to distinguish between DNA, RNA, degraded nucleic acids and other contaminants (107). Additionally, Qubit allows for detection and measurement of DNA at low concentrations, being able to read concentrations from 10 pg/µl to 100 ng/µl, making it a good instrument for this specific study.

The DNA from the different samples were quantitated by Qubit dsDNA High Sensitivity Assay Kit and the Qubit 3.0 Fluorometer according to the manufacturer's instruction. Qubit allows between 1-20 µl as input volume, and 1 µl was, therefore, used from each sample to quantitate the DNA. The equipment needed to quantitate the amount of DNA by Qubit are listed in Table 8.

Table 8 The equipment needed to perform DNA quantitation by Qubit.

Equipment	Manufacturer	Catalog Number	Lot number	Country
Qubit dsDNA High Sensitivity Assay Kit	Thermo Fischer Scientific	Q33231	2311846	USA
0.5 ml Thin-walled Tubes with flat caps	Thermo Fischer Scientific	AB-0350	60306438	USA
Biosphere® Filter Tips 0.5-20 µl	Sarstedt	70.1116.210	1051321	Germany

Eppendorf Research® plus pipette, 2-20 µl	Eppendorf	3123000098	-	Germany
Qubit™ 3.0 Fluorometer	Invitrogen	Q33216	-	USA

3.5.2 NanoDrop

To quantitate the amount of DNA, the NanoDrop One spectrophotometer was also used with its accompanying NanoDrop One software. The platform utilizes that nucleic acids absorbs light at a wavelength of 260 nm, and determines the concentration of each sample based on the amount of light that passes through the sample and the amount that is absorbed, its optical density (108). At 260/280, which is the absorbance maxima, a ratio of 1.8-2.0 is accepted as pure (109). The DNA from embryo 8 were quantitated by NanoDrop One spectrophotometer according to the manufacturer's instruction, using 1 µl from each sample. The equipment needed to quantitate the amount of DNA by NanoDrop are listed in Table 9.

Table 9 The equipment needed to perform DNA quantitation by NanoDrop.

Equipment	Manufacturer	Catalog Number	Lot number	Country
NanoDrop One Spectrophotometer	Thermo Fisher Scientific	ND-ONE-W	-	USA
Biosphere® Filter Tips 0.5-20 µl	Sarstedt	70.1116.210	1051321	Germany
Eppendorf Research® plus pipette, 2-20 µl	Eppendorf	3123000098	-	Germany

3.6 Nanopore Sequencing

In order to assess the genomic composition of the embryo biopsies, the DNA may be sequenced. Nanopore sequencing was used to test if it could be an alternative to the niPGT-A approaches, as it is investigated as a new PGT approach (95). Nanopore sequencing requires amplification of the DNA samples before they can be applied to sequencing, as the starting concentration is too low from the embryo samples, especially from the SCM samples. WGA amplification was applied by Repli-G, a multiple displacement amplification (MDA) kit, beforehand.

Only 5 embryos and their respective samples were used to perform nanopore sequencing. The embryos were chosen based on their DNA concentration, what stage they reached during the culturing and whether their dissociation was successful or not. The embryos chosen were number 11, 15, 17, 18, and 31.

3.6.1 Amplification of DNA by MDA

Amplification by MDA is based on the binding of random hexamer primers to denatured DNA, followed by strand-displacement synthesis performed by the φ29 DNA polymerase at a constant temperature (110). As the synthesis continues, the number of priming events that occur gradually increases, causing a hyperbranched network of newly synthesized DNA strands to form (Figure 8) (111). The method was developed from the multiply primed rolling circle amplification, which also utilizes the unique properties of the φ29 DNA polymerase and random primers to achieve a high-fold amplification (112). This method can yield up to 30 µg of product from as little as 1-10 copies of human DNA (110), and can also be carried out directly from biological samples making the method uniquely fitting for the low DNA quantity of the embryo biopsy samples.
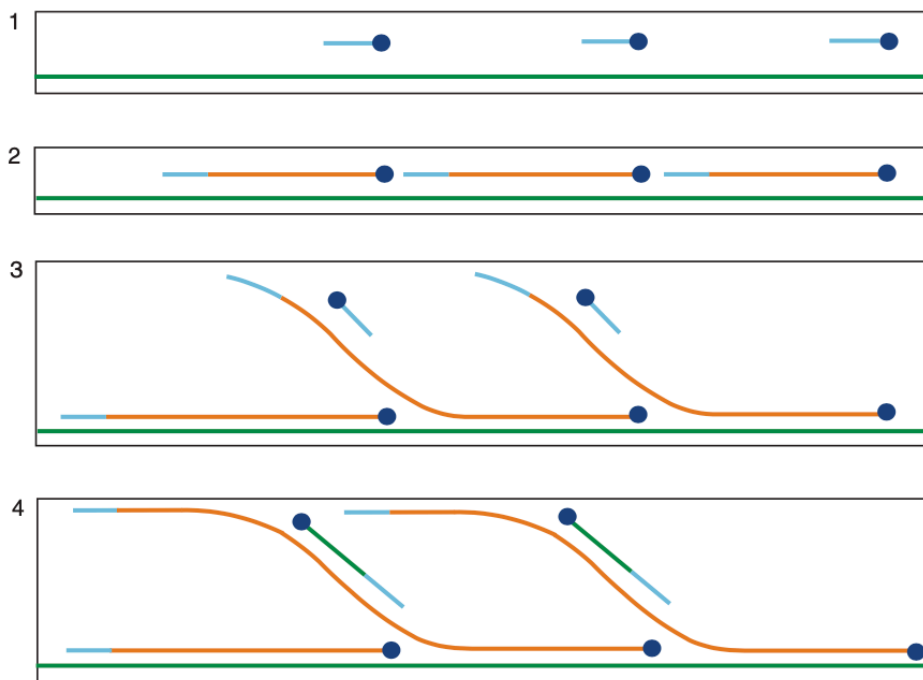
Figure 8 The principle of the multiple displacement amplification (MDA) method. *1) Random hexamer primers (blue line) anneal to the denatured DNA (green line). 2) The φ29 DNA polymerase (blue circle) extends the primes until they reach newly synthesized dsDNA (orange line). 3) The DNA polymerase then continues to displace the strand and continues with polymerization, at the same primers continue to bind to the newly synthesized DNA. 4) Polymerization starts on the newly synthesized DNA strands, forming a network of branches from the original DNA. (111)*

The DNA from the different samples were amplified by MDA using the Repli-G Single Cell Kit according to the manufacturer's instruction. Input volume from the samples were 4 μl, where the equipment needed to perform MDA are listed in Table 10 and an overview of the reagents supplied within the Repli-G single cell kit are shown in Table 11.

Table 10 Equipment needed to perform multiple displacement amplification (MDA) by Repli-G Single Cell kit.

Equipment	Manufacturer	Catalog Number	Lot number	Country
Repli-G single cell kit	Qiagen	150343	172016314, specifics listed in Table 11	Germany
DNA LoBind Tube 1.5 ml	Eppendorf	022431021	K199039N	Germany
BioClean Ultra™ 20 μl RT LTS Pipette Tips	Mettler Toledo	30389225	30729	USA
BioClean Ultra™ 200 μl RT LTS Pipette Tips	Mettler Toledo	30389239	61042	USA
Rainin Classis Pipette PR-10	Rainin	17008649	D1080682A	USA
Rainin Classis Pipette PR-100	Rainin	17008651	L0937279A	USA
Reax top vortex	VWR	444-0098	-	USA
Mini Star Silverline	VWR	3700-930	-	USA
ThermoMixer C	Eppendorf	5382000015	-	Germany

Table 11 Overview of the reagents supplied within the Repli-G single cell kit. DLB; Denaturing and lysis buffer, DTT; dithiothreitol, PBS; phosphate-buffered saline.

Reagents	Lot number
Buffer DLB	169048996
Stop solution	169047370
H_2O	172012441

DTT	1690483212
Repli-G single cell DNA polymerase	172015030
Repli-G single cell reaction buffer	169048271

3.6.2 Quantitation by Qubit and NanoDrop

The following subsections (3.6.2-3.6.4) was performed by the lab engineer at the genomic support center at UiT, due to restrictions in work regulations.

To determine the purity of the DNA in the samples after amplification by Repli-G, the samples were quantitated by NanoDrop One spectrophotometer according to the manufacturer's instruction, where 1 µl from each sample was used as input. Additionally, to determine the concentration in the samples, the samples were quantitated by Qubit dsDNA High Sensitivity Assay Kit and the Qubit 3.0 Fluorometer according to the manufacturer's instruction. As the concentration was determined to be higher than the range of concentration used in the Qubit dsDNA High Sensitivity Assay Kit, the samples were diluted 1:10 with molecular water before quantitation. 5 µl from each sample were diluted in 45 µl of molecular water, where 1 µl from these diluted samples was used as input to quantitate the amount of DNA by Qubit. The equipment needed to quantitate the amount of DNA by Qubit are listed in Table 8, while the equipment needed to quantitate the amount of DNA by NanoDrop are listed in Table 9.

3.6.3 Library Preparation

Before the samples could be sequenced using Nanopore technology, adaptors that facilitate strand capture and loading of a processing enzyme was ligated to both ends of the DNA fragments. These adaptors ensure a unidirectional displacement of the strand through the nanopore, as well as concentrating the DNA substrates at the membrane surface, heightening the DNA capturing rate (96). Additionally, the hairpin adaptor permits continuous sequencing of both strand of the dsDNA by covalently attaching the strands together. This was performed during the library preparation, where the ligation sequencing kit and the native barcoding kit were used. Barcoding was used to be able to pool the samples together during the run of the flow cell. Long-fragment buffer was used during the library preparation, instead of short-fragment buffer.

For each sample, a calculation was made to get the right amount of DNA diluted with water to obtain an input of 1000 ng DNA. After barcoding had finished, the samples were quantitated once more to calculate the right amount needed to obtain an input of 80 ng in each sample to make the pooled input of 800 ng DNA before sequencing.

The library preparation of the samples was performed by the ligation sequencing kit and the native barcoding kit according to the manufacturer's instruction, expect a qPCR machine was used instead of a thermal cycler. The equipment used to perform the library preparation are listed in Table 12 and Table 13, while the reagents used are listed in Table 14.

Table 12 Equipment used to perform the library preparation for the embryo samples to be sequenced using Oxford Nanopore Technologies.

Equipment	Manufacturer	Catalog Number	Lot number	Country
Ligation sequencing kit XL	Oxford Nanopore Technologies	SQK-LSK109-XL	10.0002, specifics listed in Table 13	UK
Flow cell priming kit	Oxford Nanopore Technologies	EXP-FLP002	10.0017, specifics listed in Table 13	UK
Native barcoding expansion 1-12	Oxford Nanopore Technologies	EXP-NBD104	EN04.10.0016	UK
NEBNext Companion Module for Oxford Nanopore Ligation Seuquencing	New England BioLabs	E7180S	10128600	USA
Biosphere® Filter Tips 0.5-20 µl	Sarstedt	70.1116.210	1051321	Germany
Eppendorf Research® plus pipette, 2-20 µl	Eppendorf	3123000098	-	Germany
HulaMixer sample mixer	Thermo Fisher Scientific	15920D	-	USA
Microseal ´B´ Seal	Bio-Rad	MSB1001	B0135833	USA
Hard-Shell PCR-plates 96-well low	Bio-Rad	HSL9901	20130114	USA

profile, semi-skirted				
CFX96 Real-Time PCR system	Bio-Rad	1855196-8005174723-000170-1	-	USA
CFX Maestro software	Bio-Rad	-	-	USA

Table 13 Overview of the contents of the "ligation sequencing kit" and the "flow cell priming kit" from Oxford Nanopore Technologies.

Reagents	Lot number
Flush buffer	SK1581016
Flush tether	SK13102003
Loading beads	SK1271002XL
Sequencing buffer	SK1281002XL

Table 14 Overview of the reagents needed to perform library preparation.

Reagents	Manufacturer	Catalog Number	Lot number	Country
AMPure XP	Beckman Coulter	A63081	18470700	USA
Blunt/TA ligase mastermix	New England BioLabs	M0367L	10104494	USA

3.6.4 Sequencing

Once the library preparation was done, the flow cell could be applied to the GridION machine for nanopore sequencing. During the sequencing the DNA molecules are captured by the nanopores, where they are processed through the pore while a sensor detects changes in the ionic current caused by the pore being occupied by different nucleotides. These ionic current changes are then separated as discrete events with their associated duration, variance, and mean amplitude, which can be interpreted computationally as a sequence of 3-6 nucleotide long words called "kmers" by using graphical models. Each strand is sequenced with a "template

read" and a "complement read", which can be combined to produce a "2D read" using pairwise alignment of the events (96).

After the samples had been pooled together in two parallels during the library preparations, the two parallels were quantitated by Qubit to determine the right amount needed to run on the flow cell. The concentration needed depends on the length of fragments, thus, given that the fragment lengths are unknown in half the samples, half of the normal input volume was used. 6 µl was, therefore, used as input from the first pooling mixture while the remaining 6 µl was taken from the elution buffer, this gave a concentration of 167 ng/µl of the pooled sample on the flow cell.

The nanopore sequencing was performed by GridION Mk1 according to the manufacturer's instruction. The equipment used to sequence the samples are listed in Table 15.

Table 15 Equipment used to perform nanopore sequencing on the embryo biopsies.

Equipment	Manufacturer	Catalog Number	Lot number	Country
Flow Cell R9.4.1	Oxford Nanopore Technologies	FLO-MIN106D	FAS78047	UK
GridION™ Mk1	Oxford Nanopore Technologies	-	-	UK
MinKNOW v.21.11.7	Oxford Nanopore Technologies	-	-	UK

3.6.5 Processing of the Sequencing Data

The following subsection was performed by the post-doctoral fellow in clinical bioinformatics at the genomic support center at UiT.

Once sequencing had finished, the data output from the GridION could be processed. The file format of the data from nanopore is fast5, which can be converted to fastq after basecalling. Basecalling is a translation of the raw signals into segments with information about current level, noise level and duration corresponding to the movement of DNA through the pore. The passed fastq files were then aligned to the human genome assembly 38 (Hg38) using the minimap2 algorithm. The resultant sam-files were converted into bam-files and indexed with

samtools, which extracts alignments overlapping particular genomic regions. The reads were then converted to genomic ranges with the R chromstaR readBamFileAs GRanges function. From there, all manipulation was done with the GenomicRanges package. The R GenomicAlignments package and R msa package was used to create the consensus sequence, which was searched against the human genome using blastn. Finally, the heatmap.2 function from the R gplot package was used to create the heatmap.

3.7 Target Specific Amplification by ddPCR

Amplification by ddPCR is based on a water-oil emulsion technology, where the sample is fractionated into 20 000 droplets before the conventional TaqMan assay can be applied to amplify the contents of each individual droplet in a PCR reaction (113). This method is especially good for locating and amplifying a specific target gene in a bigger gene pool, allowing a target sequence to be amplified in reference to another gene. Because of this localization of genes, the target genes can be specified to known genetic diseases, such as trisomy 21, by selecting genes known to be present on chromosome 21. In this study, two sets of FAM TaqMan hydrolysis assays were used to target *runt related transcription factor 1* (*RUNX1*) and *bromodomain and WD repeat domain containing 1* (*BRWD1*), which are two of the same genes used in a proof-of-concept paper for a non-invasive alternative to prenatal testing of trisomy 21 using ddPCR (114). For the reference genes two VIC TaqMan hydrolysis assays that target *transcription factor 4* (*TCF4*) and *SMAD family member 4* (*SMAD4*) were used, which also were included in the same paper (114). These genes are located on chromosome 18 to function as both a reference and a possible trisomy 18 marker.

3.7.1 Performing ddPCR

ddPCR utilizes an eight-well droplet generating cartridge where the oil and the sample, together with ddPCR supermix and the TaqMan reagents, are loaded onto the eight individual wells of the cartridge (Figure 9). Once the cartridge is loaded, a vacuum is applied to the wells, drawing both the oil and the sample through a flow-focusing junction generating uniform droplets at a rate of ~1000 per second. These newly formed droplets flow to the collection well where they form a densely packed bed, allowing for their transfer over to a conventional 96-well PCR plate for thermal cycling. To establish the absolute concentration of the target sequences, the plate is then transferred to a droplet reader. During the reading of the droplets, they are streamed towards a detector with a spacer fluid that separates them and aligns them for detection of the specific duplexed coloring of the reference and target DNA probes provided by the TaqMan

assay. Each droplet containing the template have specific cleavage of the TaqMan probes, generating a strong fluorescent signal. Based on the amplitude of the fluorescent signals, a simple threshold is used to assign the droplets as positives or negatives. As the volume of each droplet is known, the portion of positive droplets can then be used to calculate the absolute concentration of the target DNA (113).
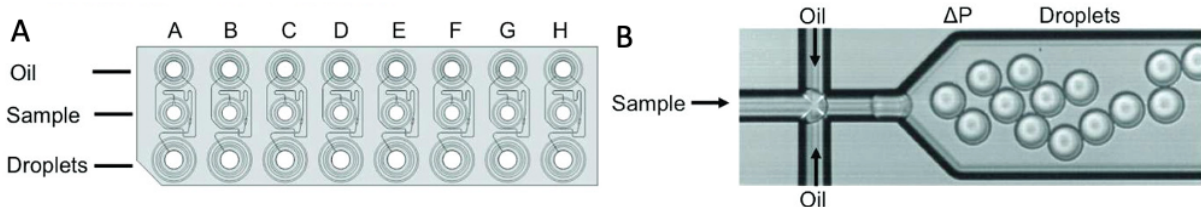
Figure 9 The setup of the eight-well droplet generating cartridge used in ddPCR. *A) The cartridge consists of eight wells on each row, with each row containing a different reagent: one for the oil, one for the sample and one for the created droplets. The samples and oil are loaded onto the cartridge, and then during the ddPCR the droplets are formed and amplified in the last row. B) Vacuum is applied to the wells making both the oil and the sample drawn through a flow-focusing junction where the monodispersed droplets are generated. ddPCR; digital droplet PCR. Modified from (113).*

The setup of reagents and the samples is presented in Table 16. In each sample-well there is a total of 20 µl, which includes 6 µl of DNA from the sample and 14 µl of the ddPCR reagents. This gave a final concentration of 125 nM for the probes and a final concentration of 450 nM for the primers. In the oil wells, 70 µl of droplet generating oil was added to each. Each sample was run in duplicate.

Table 16 Overview of the reagent setup in the ddPCR reaction well. *The assays used as reference were transcription factor 4 (TCF4) and SMAD family member 4 (SMAD4), whilst the assays used as target were runt related transcription factor 1 RUNX1) and bromodomain and WD repeat domain containing 1 (BRWD1).*

ddPCR Setup	Amount (µl)
Supermix	10
TCF4 assay	0.5
SMAD4 assay	0.5
RUNX1 assay	0.5
BRWD1 assay	0.5
Sterilized H_2O	2
Total volume	14
+	
DNA	6

After the sample and the droplet generating oil had been added, they were put into the droplet generator. 40 µl of the generated droplets from each sample was transferred to the PCR-plate using a multichannel pipet and run on the thermal cycling program presented in Table 17. The

thermal cycling program is the standard thermal cycling program used for ddPCR and the same program was used in the study from 2016 which had the same TaqMan assays (114).

Table 17 The PCR thermal cycling program used to perform the target specific amplification. The program is the standard thermal cycling program used for digital droplet PCR (ddPCR).

PCR Thermal Cycling Program		
	Temperature (°C)	Time (Sec)
Initial hot start	95	600
Steps 1 and 2 are repeated through 40 cycles		
Step 1	94	30
Step 2	60	60
Step 3	98	600
Step 4	12	Infinity

ddPCR was performed by the QX200 System and its associated applications and accessories according to the manufacturer's instruction. The equipment used to amplify the DNA samples by ddPCR are listed in Table 18 and the reagents used are listed in Table 19.

Table 18 Equipment used to perform digital droplet PCR (ddPCR).

Equipment	Manufacturer	Catalog Number	Lot number	Country
Multiply -µStrip 0.2 ml chain	Sarstedt	72-985.002	8082111	Germany
Biosphere lid chain, flat	Sarstedt	65.989	8081711	Germany
BioClean Ultra™ 200 µl RT LTS Pipette Tips	Mettler Toledo	30389239	61042	USA
BioClean Ultra™ 20 µl RT LTS Pipette Tips	Mettler Toledo	30389225	30729	USA
Rainin Classis Pipette PR-10	Rainin	17008649	D1080682A	USA

Rainin Classis Pipette PR-100	Rainin	17008651	L0937279A	USA
DG8™ Cartridges for GX200™ Droplet Generator	Bio-Rad Laboratories	1864008	1000122047	USA
DG8™ Cartridges Holder	Bio-Rad Laboratories	1863051	-	USA
DG8™ Gaskets for QX200™ Droplet Generator	Bio-Rad Laboratories	1863009	20211018	USA
Pipet-Lite Multi Pipette L12-200XLS+	Rainin	17013810	C044371329	USA
ddPCR™ 96-Well Plates	Bio-Rad Laboratories	12001925	64437535	USA
PCR Plate Heat Seal, foil, pierceable	Bio-Rad Laboratories	1814040	101719	USA
QX200™ Droplet Generator	Bio-Rad Laboratories	1864002	-	USA
PX1 PCR Plate Sealer	Bio-Rad Laboratories	1814000	-	USA
T100™ Thermal Cycler	Bio-Rad Laboratories	1861096	-	USA
QX200™ Droplet Reader	Bio-Rad Laboratories	1864003	-	USA
Droplet Reader Waste Bottle	Bio-Rad Laboratories	N/A	-	USA
QuantaSoft™ Software, version 1.7, regulatory edition	Bio-Rad Laboratories	1864011	-	USA
QX Manager Standard Edition, Version 1.2	Bio-Rad Laboratories	-	-	USA

Table 19 Reagents used to perform digital droplet PCR (ddPCR).

Reagents	Manufacturer	Catalog Number	Lot number	Country
ddPCR Supermix for Probes (no dUTP)	Bio-Rad Laboratories	1863024	64416794	USA
Hs00372815_cn, TCF4	Thermo Fisher Scientific	4400291	P220121-005 E11	USA
Hs06447834_cn, SMAD4	Thermo Fisher Scientific	4400291	P220121-005 E10	USA
Hs03026207_cn, BRWD1	Thermo Fisher Scientific	4400291	P220121-005 E09	USA
Hs05550012_cn, RUNX1	Thermo Fisher Scientific	4400291	P220121-005 E08	USA
Droplet Generation Oil for Probes	Bio-Rad Laboratories	1863005	64445379	USA
ddPCR™ Droplet Reader Oil	Bio-Rad Laboratories	1863004	64452384	USA

4   Results

4.1   Long-Term Storage Gave a Higher Quantity of Viable Day 5 Embryos

In total, 36 embryos were retrieved from long-term storage and thawed to use in this study. Out of the 36, the first seven embryos thawed were used to acquire the necessary techniques to handle, culture, and dissociate the embryos. Embryos frozen on both day 3 and day 5 were thawed throughout the study, where there was a visible trend with embryos frozen on day 5 being of higher quality and being less fragmented than those frozen on day 3 (Table 20). Even though the majority of the embryos were viable and had continuous development after thawing, $1/4^{th}$ of the day 3 embryos were heavily fragmented and, thus, terminated within the first 48 hours after thawing. Contrastingly, only $1/8^{th}$ of day 5 embryos thawed were heavily fragmented and terminated within the first 48 hours after thawing.

Table 20 An overview of the number of fragmented and non-fragmented embryos after thawing, according to their developmental stage.

Embryo Stage	Non-Fragmented	Fragmented	Total Number of Embryos	Fraction
Day 3	9	3	12	$1/4^{th}$
Day 5	21	3	24	$1/8^{th}$

During the incubation of the different embryos used in this study, pictures were taken to demonstrate their development, assess their morphology, and assign them a score according to the Istanbul criteria (Appendix D). The images taken of the embryos clearly show how the embryo develops from having a few blastomeres right after thawing (Figure 10;A), to the blastomeres increasing in number while decreasing in size to form a morula (Figure 10;B,C). They also show the process of compaction, where the blastomeres lose their individuality and maximize their cell-cell junctions (Figure 10;D), to when blastulation occurs and fluid starts to penetrate the zona pellucida to form an early blastocyst (Figure 10;E). Finally, the fully expanded blastocyst is visible (Figure 10;F) where the ICM is clearly distinct from the thin outer layer of the TE. Once the blastocyst has expanded to the zona pellucida's maximum capacity, the glycoprotein membrane disrupts, initiating the hatching of the embryo (Figure 10;G) to prepare for implantation. Embryo 2 is pictured in Figure 10;A, embryo 34 is pictured in Figure 10;B-F, and embryo 15 is pictured in Figure 10;G.
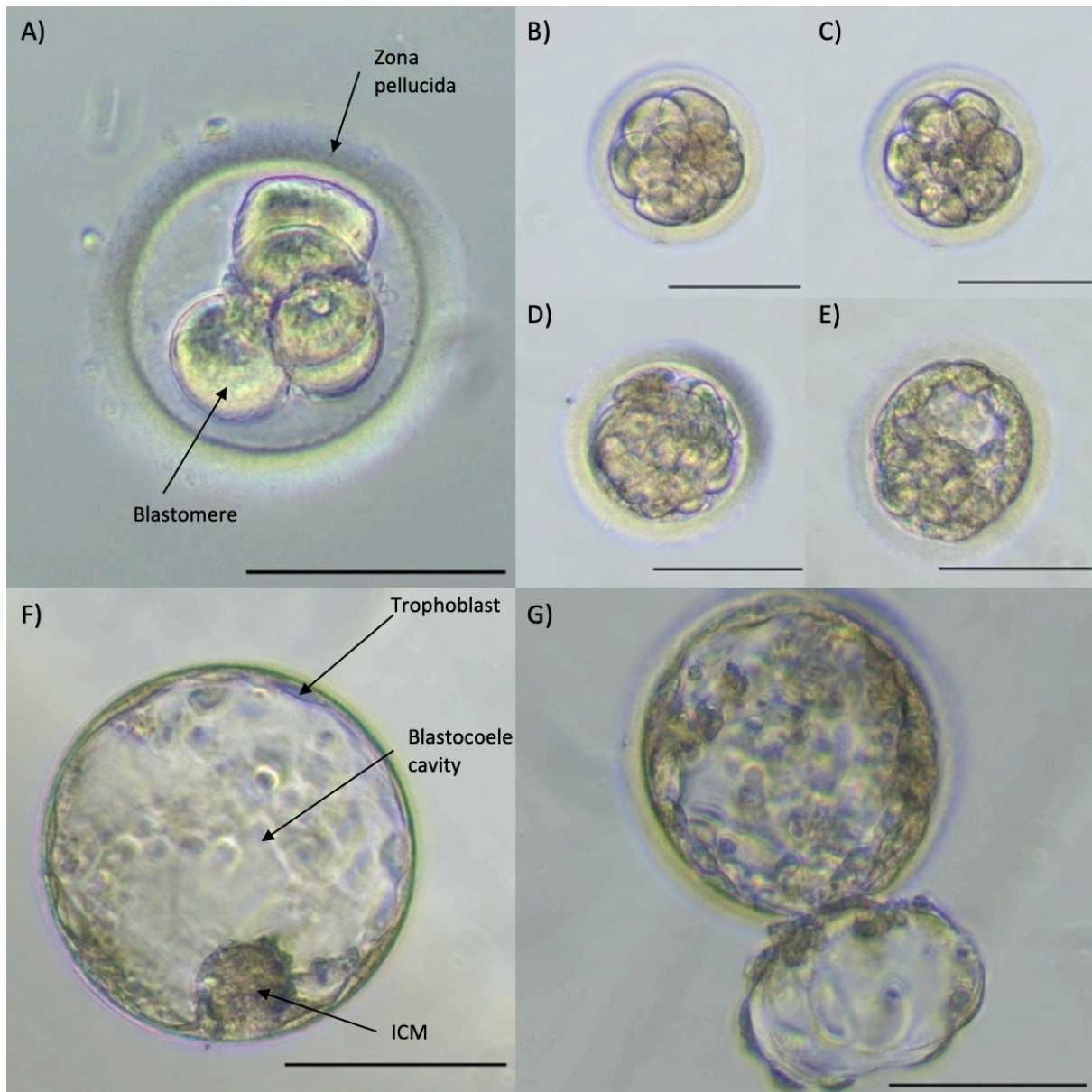
Figure 10 Images taken throughout the development of an embryo. *A) Image of the embryo on day 2, with 4 blastomeres and a clear zona pellucida. B-D) The development of the embryo from late day 2/early day 3 to early day 4, with the number of blastomeres increasing (B), the morula forming (C) and compaction ensuing (D). E) Blastulation starts as fluid penetrates the zona pellucida on day 4 and an early blastocyst forms, dividing the blastomeres into the two cell lineages; inner cell mass (ICM) and the trophoectoderm (TE). F) The fluid continues to penetrate the zona pellucida expanding the embryo into a fully developed blastocyst on day 5, with a clear ICM and a thin TE, with the zona pellucida at its thinnest as well. G) On day 6, hatching has started, and the embryo is slowly shedding the zona pellucida as the embryo continues to expand in size. The images were captured using DeltaPix HDMI 16MDPX camera and the scale bar is set to 100 μm.*

4.2 Successful Dissociation of the Blastocyst Leaves the Zona Pellucida Intact with Single or Cluster of Cells in the Surrounding Media

The embryos were observed under the microscope during the dissociation, where images were taken to demonstrate how the two cell lineages were undistinguishable from each other once they were dissociated from the zona pellucida (Figure 11). After dissociation, the zona pellucida is still intact, whereas the cells are either single or in a cluster of cells in the surrounding media.
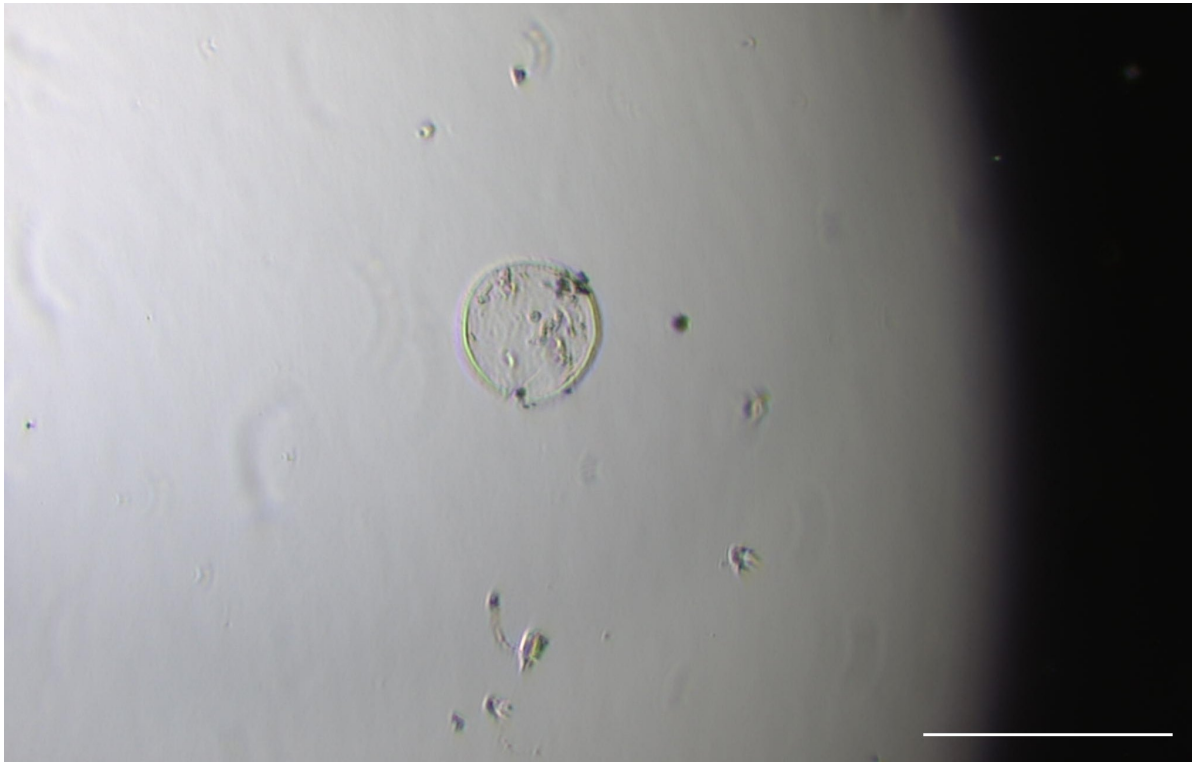
Figure 11 Image of an embryo in the process of being dissociated, leaving the cells removed from the zona pellucida. *The zona pellucida is still intact and almost empty, with single cells or clusters of cells being visible in the surrounding media. The image was captured using DeltaPix HDMI 16MDPX camera and the scale bar is set to 100 μm.*

4.3 More DNA was Found in 3/4ᵗʰ of the Samples Derived from Whole Blastocyst Biopsies than Samples Derived from SCM Biopsies

Qubit determined the DNA concentration in ng/μl, and the concentrations determined in the different samples are presented in Table 21. The sample name consists of two numbers, the first represents the embryo and the second represents the biopsy type (x.1 indicates SCM biopsies and x.5 whole blastocyst dissociation samples). Every sample had DNA present, with a mean of 1.289 ng/μl throughout the samples, indicating the presence of cfDNA in the SCM samples and DNA in the dissociated embryo samples. Eight embryos (embryos 8, 15, 25, 27, 29, 32, 34, and 36), out of 29, had higher concentrations of DNA present in their SCM samples than in their whole blastocyst dissociation samples.

Table 21 Overview over the different embryo-biopsies and their corresponding DNA concentrations measured on Qubit. *The first number in the sample name indicates the embryo which the sample was taken from, and the second number represent what type of biopsy was taken; x.1 indicates a whole embryo dissociation biopsy and x.5 indicates a spent culture media (SCM) biopsy.*

Sample Name	DNA concentration (ng/μl)	Sample Name	DNA concentration (ng/μl)
E8.1	0.872	E22.5	1.20

E8.5	0.574	E23.1	0.922
E9.1	0.806	E23.5	1.08
E9.5	0.972	E24.1	0.682
E10.1	0.78	E24.5	6.94
E10.5	0.934	E25.1	0.622
E11.1	0.748	E25.5	0.23
E11.5	1.01	E26.1	1.27
E12.1	0.664	E26.5	1.62
E12.5	0.846	E27.1	0.602
E13.1	0.366	E27.5	0.32
E13.5	0.383	E28.1	0.59
E14.1	0.832	E28.5	1.41
E14.5	1.46	E29.1	0.356
E15.1	1.08	E29.5	0.118
E15.5	0.898	E30.1	0.41
E16.1	0.976	E30.5	0.876
E16.5	1.12	E31.1	0.50
E17.1	0.93	E31.5	8.26
E17.5	1.06	E32.1	4.84
E18.1	0.864	E32.5	0.946
E18.5	1.33	E33.1	0.67
E19.1	1.0	E33.5	5.48
E19.5	1.24	E34.1	3.62
E20.1	1.12	E34.5	0.888
E20.5	1.24	E35.1	1.33
E21.1	0.26	E35.5	5.28
E21.5	1.17	E36.1	2.48
E22.1	0.57	E36.5	1.42

Only the two samples from embryo 8 were quantitated using NanoDrop, where the concentration was determined in ng/µl and the results are listed in Table 22. The two samples that were quantitated using NanoDrop had concentrations of 122.35 ng/µl and 193.05 ng/µl and were from a SCM biopsy and a whole blastocyst dissociation, respectively. These values are higher than excepted and higher than the DNA concentrations determined for the same samples by Qubit.

Table 22 Overview of the measured DNA concentrations for both samples from embryo 8 performed on NanoDrop.

Sample Name	DNA concentration (ng/µl)	Absorbance Ratio 260/280	Absorbance Ratio 260/230
E8.1	122.35	3.38	0.151
E8.5	193.05	3.39	0.13

NanoDrop also measures absorbance, which is a measure of purity. The purity of the DNA is determined by which wavelength the light is absorbed at (109). An absorbance ratio of 1.8-2.0 is normally considered pure at 260/280, whereas a ratio of 2.0-2.2 is accepted for 260/230. The absorbance ratios measured for the two samples were at ~3.4 for both samples at 260/280 and at ~0.1 for both samples at 260/230 (Table 22). These values are not in the accepted range of purity, indicating either contamination in the samples or decreased sensitivity to lower concentrations by the instrument.

4.4 Repli-G Amplification of Embryo DNA Gave Over a Thousandfold Increase in Concentration

After amplification by Repli-G, the samples with the amplified DNA were quantitated by NanoDrop to determine the purity of the samples and by Qubit to determine the amount of DNA in each sample.

NanoDrop determined the DNA concentration in ng/µl and the corresponding absorbance ratios at 260/280 and 260/230, the values determined in the samples after amplification by Repli-G are presented in Table 23. As mentioned, an absorbance ratio of 1.8-2.0 is normally considered pure at 260/280, whereas an absorbance ratio of 2.0-2.2 is accepted for 260/230. All the samples measured by NanoDrop were within the accepted range for both absorbance ratios, indicating purity and good quality in all of the samples. The concentration determined by NanoDrop showed a huge increase from the concentration determined in the samples before amplification, increasing from a mean of 1.289 ng/µl before amplification to a mean of 2099.29 ng/µl after amplification. This equals a fold increase of 1627.57, indicating that the amplification of DNA from the embryo-derived samples was successful.

Table 23 Overview of the DNA concentrations and the corresponding absorbance ratios determined by NanoDrop in the samples after amplification by Repli-G.

Sample Name	DNA concentration (ng/µl)	Absorbance Ratio 260/280	Absorbance Ratio 260/230
E11.1	2051.9	1.89	2.02
E11.5	2135.8	1.83	2.04
E15.1	2170.2	1.85	2.05
E15.5	1964.7	1.81	2.01
E17.1	2062.5	1.86	2.05
E17.5	2157.0	1.88	2.06
E18.1	2070.8	1.90	2.08
E18.5	2090.5	1.82	2.03
E31.1	2078.7	1.89	2.20
E31.5	2210.8	1.85	2.16

Qubit determined the DNA concentration in ng/µl and the concentration determined in the different samples that were amplified by Repli-G are presented in Table 24. The concentrations determined by Qubit showed successful amplification compared to the concentrations measured before amplification, even with 1:10 dilution.

Table 24 Overview of the DNA concentrations determined by Qubit in the samples after amplification by Repli-G.

Sample Name	DNA concentration (ng/µl)
E11.1	84.4
E11.5	71.2
E15.1	81.2
E15.5	60.8
E17.1	76.8
E17.5	92.0
E18.1	89.8
E18.5	71.2
E31.1	81.8
E31.5	75.4

4.5 DNA Concentrations After Library Preparation and Barcoding Were Consistent Throughout the Samples

The samples were quantitated once more after barcoding had finished, both to ensure successful separation of the DNA from the magnetic beads during library preparations, but also to calculate

the necessary amount of DNA from each sample before pooling. Qubit determined the DNA concentration in ng/µl and the concentration determined in the samples after barcoding are presented in Table 25. The samples show good consistency with the concentrations ranging from 19 ng/µl to 26 ng/µl.

Table 25 Overview of the DNA concentrations determined by Qubit in the samples after barcoding in preparation for nanopore sequencing.

Sample Name	DNA concentration (ng/µl)
E11.1	22.0
E11.5	21.2
E15.1	19.4
E15.5	26.0
E17.1	20.4
E17.5	19.1
E18.1	21.4
E18.5	19.1
E31.1	21.4
E31.5	21.8

4.6 Nanopore Sequencing May be Used for Investigation of cfDNA Secreted from Embryos

Before the sequencing a total of 1445 pores were detected, whereas for the second run a remaining 1068 pores were detected after the blocked pores were washed. The samples ended up successively blocking the nanopores over the course of the first three hours of the sequencing on both runs, limiting the data output generated. Yet, enough data was produced to analyze the 50 biggest differences in read counts for chromosome 21 and 18. A consensus sequence was generated from a genomic block of overlapping reads and verified by a genomic blastn search. In embryo 11 a correlation was found for overlapping regions between the samples.

Table 26 presents an overview of the sequencing data, where the number of reads per sample is presented, as well as the mean read length and the longest read in bp for the samples. The numbers of reads generated ranged from 7607 to 90 632. Overall, the generated number of reads per sample is insufficient to use the reads to find any reliable data concerning the genomic state of the embryos. The mean read length ranged from 451 bp to 1799 bp, where all samples obtained a higher mean read length in their whole blastocyst dissociation sample than in their

SCM biopsy sample. Furthermore, the longest read in the samples ranged from 11 759 bp to 21 306 bp.

Table 26 An overview of the sequencing data, highlighting the number of reads per sample, the mean read length and the longest read in bp per sample. Samples taken from the spent culture media (SCM) are represented by x.1, while samples taken of the whole dissociated blastocyst are represented by x.5.

Sample Name	Number of Reads	Mean Read Length (bp)	Longest Read (bp)
E11.1	48 390	451.61	11 759
E11.5	40 039	1799.39	20 481
E15.1	11 910	1101.63	19 934
E15.5	17 554	1767.77	20 402
E17.1	90 632	606.25	14 661
E17.5	7607	1082.37	13 721
E18.1	79 025	501.42	18 122
E18.5	51 285	1550.50	17 335
E31.1	74 072	720.76	21 306
E31.5	36 630	1752.63	17 398

With the sequencing run being shortened, there were some clear differences in the read counts between the two samples originating from the same embryo. The 50 biggest differences in read counts for the two samples from the same embryo have been highlighted in heatmaps for both chromosome 21, presented in Figure 12, and chromosome 18, presented in Figure 13. The red color represents a higher read count in the SCM biopsy sample (x.1) than in the whole blastocyst dissociation sample (x.5), whereas the blue color represents a higher read count in the whole blastocyst dissociation sample than in the SCM biopsy sample.

For chromosome 21, there was a generally higher read count in the SCM biopsy samples for embryo 11, 17, and 31, whereas embryo 15 and 18 had more read counts in the whole blastocyst dissociation samples. For chromosome 18, there was generally a higher read count in the SCM biopsy samples for all embryos than in the whole blastocyst dissociation samples. With these large differences in the read counts between the different biopsy samples from each embryo, a comparison of the genetic contents in each embryo cannot be done. There is no way to tell if there is an overlap between the biopsies without having a greater read count, and, thus, further

investigation into the optimization of this method is needed to generate a better foundation for downstream analysis and application.

Embryo 15 had the fewest number of reads in total for its samples, which might explain why there were only a few differences detected between the read counts from each sample in the heatmap for both chromosome 18 and 21. Similarly, embryo 17 had quite a high number of reads in the SCM biopsy sample compared to its whole blastocyst dissociation sample, which might explain why the majority of the differences in read counts are favored for the SCM biopsy samples in both chromosome 18 and 21.
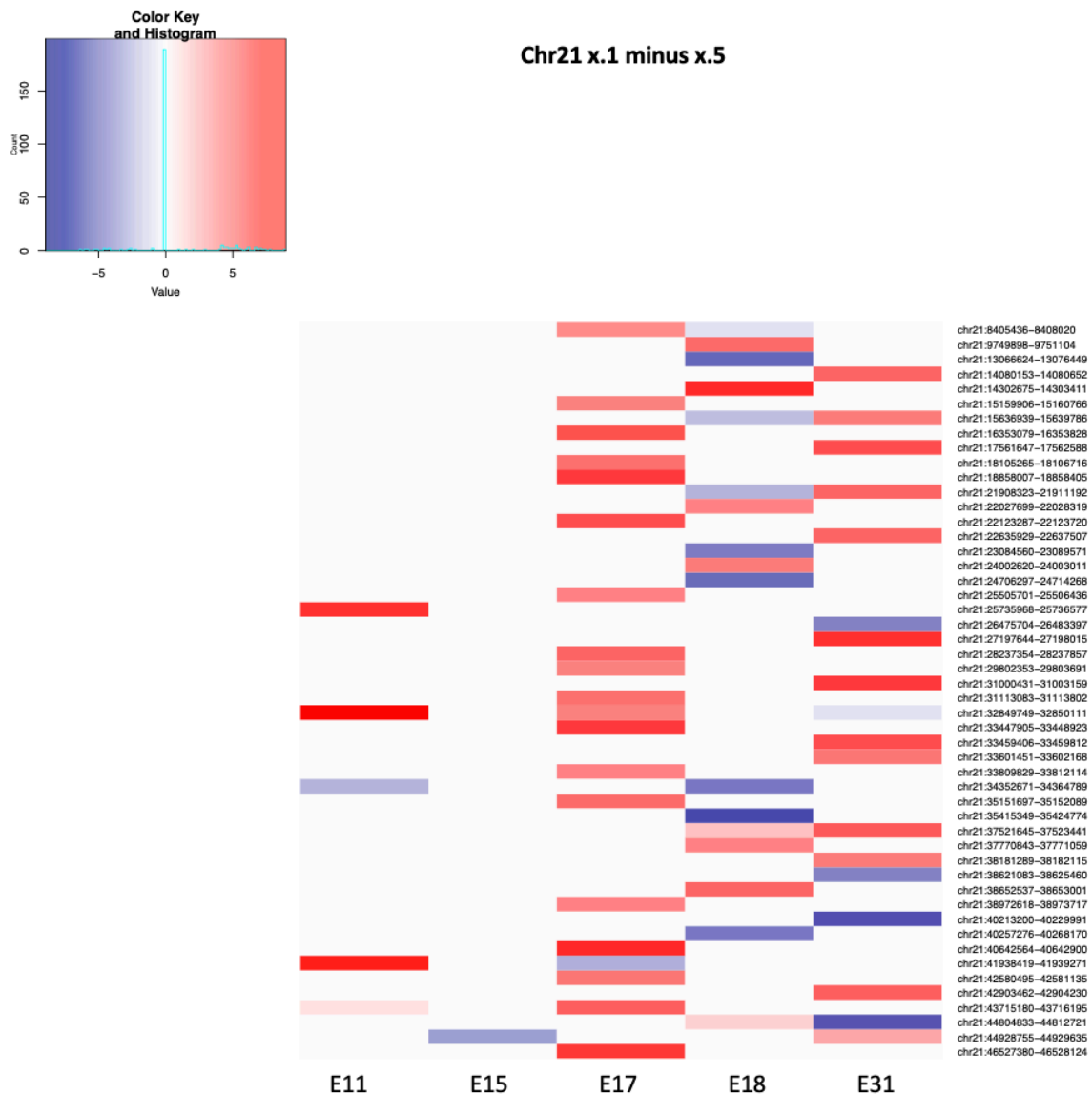
Figure 12 Heatmap highlighting the 50 biggest differences between the read counts for the two samples from the same embryo have been highlighted for chromosome 21. *Red represents more read counts in the spent culture media (SCM) biopsy samples (x.1), whereas blue represents a higher read count in the whole blastocyst dissociation samples (x.5). Embryos 11, 17 and 31 had a generally higher read count for their SCM biopsy samples, while embryos 15 and 18 had a higher read count in their whole blastocyst dissociation samples.*
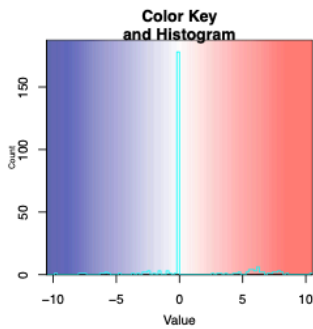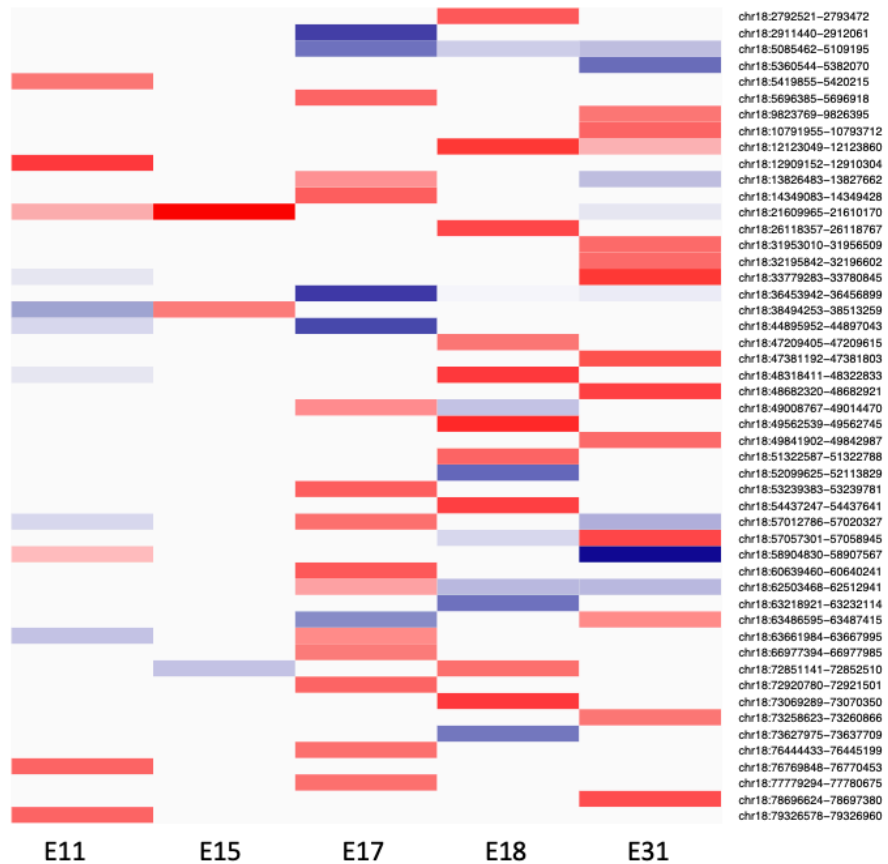
Figure 13 Heatmap highlighting the 50 biggest differences between the read counts for the two samples from the same embryo have been highlighted for chromosome 18. *Red represents more read counts in the spent culture media (SCM) biopsy samples (x.1), whereas blue represents a higher read count in the whole blastocyst dissociation samples (x.5). There is generally a higher read count for the SCM biopsy samples than for the whole blastocyst dissociation samples for all five embryos.*

The +-strands from the overlapping reads for sample E18.1 on chr10:93044437-9309483 was aligned to generate a consensus sequence, presented in Figure 14. The consensus sequence was verified by using blastn to search against the human genome (Appendix E). This search found the sequence to align correctly with the genome at the right location, indicating that the data contains real DNA sequences, just that the sequencing did not produce enough data to do a greater analysis with. However, sample E18.1 is a SCM sample and the fact that the consensus sequence aligns to the human genome shows great promise to the use of cfDNA found in the SCM to analyze the embryos.
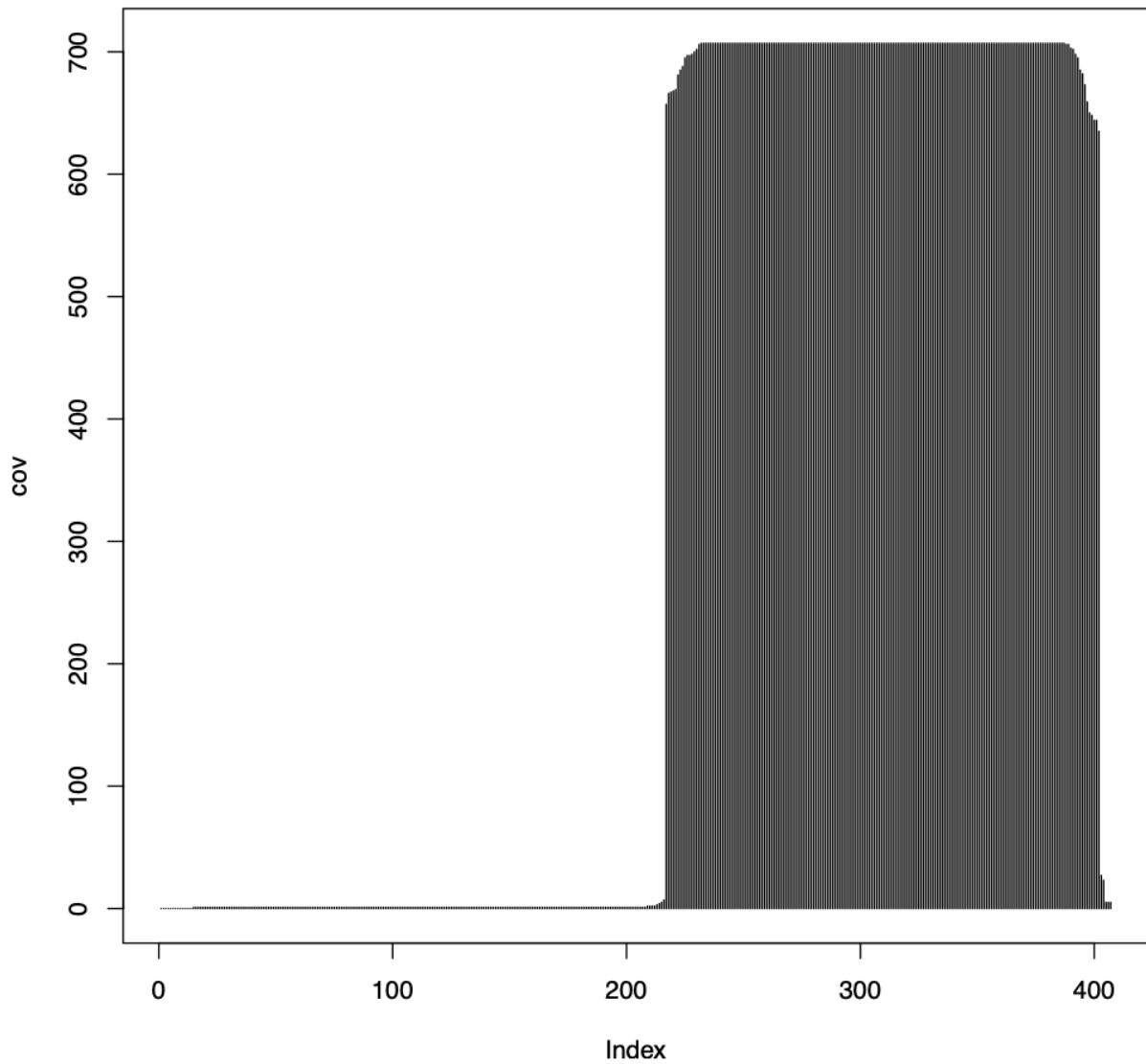
Figure 14 A representation of the +-strands from the overlapping reads for sample E18.1 on chromosome 10. *These overlapping reads was used to generate a consensus sequence, which revealed correct alignment to the human genome at the right location, indicating real DNA from the samples. The x-axis represents the index, the order of the reads, whereas the y-axis represents the coverage of the reads.*

There was only one embryo that had reads within the same region, embryo 11. The overlapping read counts from the two samples E11.1 and E11.5 within the same region on chromosome 3 is presented in Figure 15. The number of overlapping reads were 29, where the correlation for the overlapping regions, i.e., reads present in both samples, was 0.41. Embryo 11 was the only sample that gave a decent correlation, which is probably due to the limited number of reads generated from the sequencing.

correlation (0.41) overlapping reads n=29

chr3:134221027–134221523
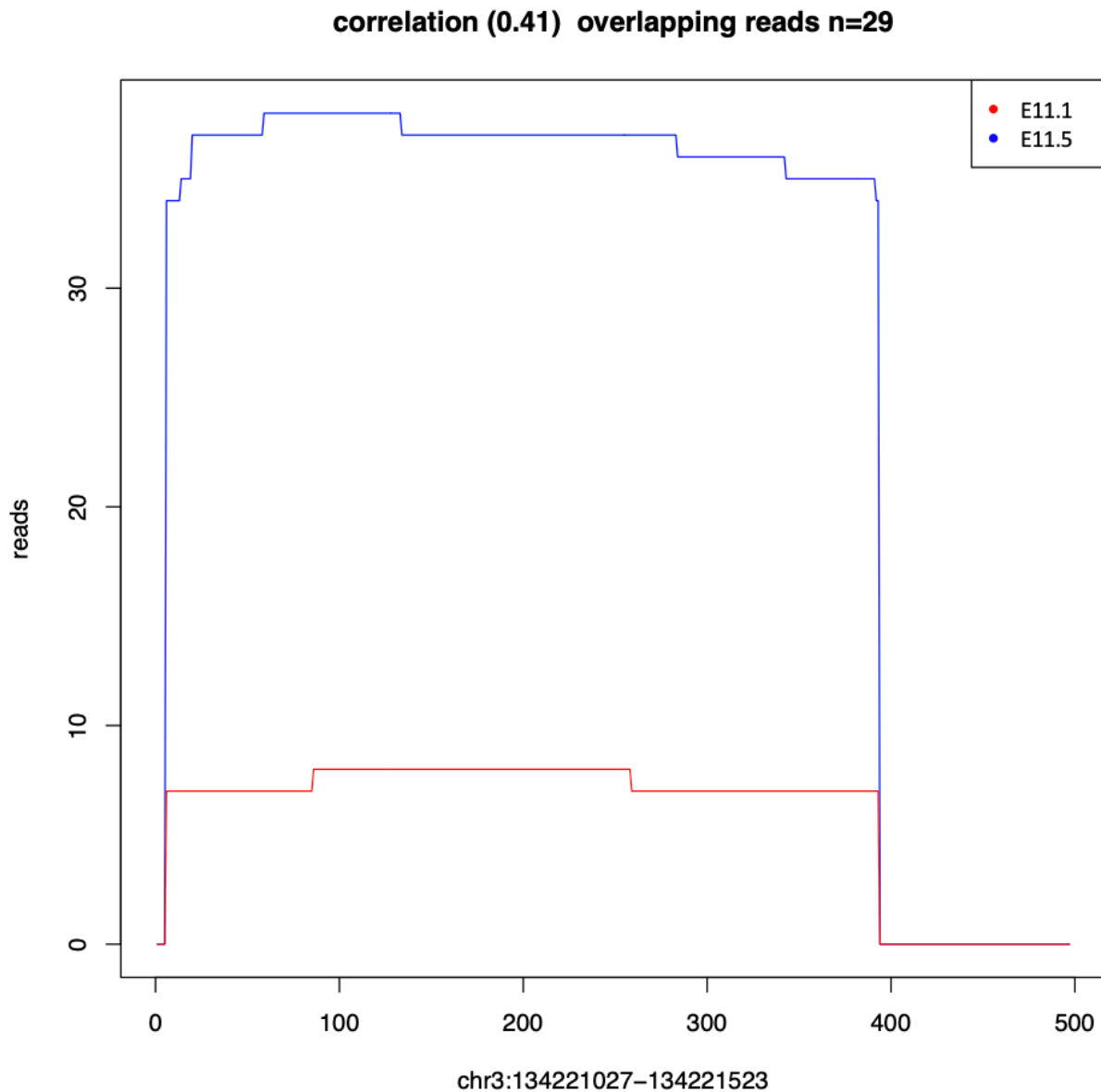
Figure 15 A presentation of the reads that where within the same region for both samples of embryo 11. The number of overlapping reads were 29, where the overlapping correlation was 0.41. The region in question is located on chromosome 3. E11.1 represents the sample taken from the spent culture media (SCM), while E11.5 represents the sample taken of the whole dissociated embryo.

4.7 ddPCR Detected Genes Involved in Trisomy 21 from Biopsies Taken from the SCM Containing cfDNA

Due to insufficient detection of either probe in the VIC channel targeting the reference genes *TCF4* and *SMAD4* located on chromosome 18, only a single run containing samples from embryos 19, 20, 21, 26, 28, 33, 34, 35, and 36 were used to perform ddPCR.

The generated number of droplets in the samples ranged from 7315 to 13 562, with a mean of 11 200 droplets generated throughout the samples. 10 000 droplets are considered the threshold for accepted number of droplets, where any less than that are most likely due to the wrong

concentration of the supermix, assays, or loss of droplets during transfer. There were 6 samples from separate duplicates that were below this accepted threshold, these were from the duplicates of samples E19.1, E28.1, E28.5, E33.1, E33.5, and E35.1. Despite the lower number of droplets generated, there were still positive droplets to be found in three of these duplicates (E28.1, E33.5 and E35.1).

Each droplet generated contains a small portion of the sample, where only the droplets containing the target DNA will give a positive droplet once the probe binds and a fluorophore is detected. Only samples E19.1, E20.1, E21.1, E26.1, E26.5, E28.1, E33.5, E34.1, E35.1, E36.1, and E36.5 had positive droplets detected, where the number of positive droplets generated in the duplicates ranged from 6 to 72 (Figure 16 and Figure 17). The number of positive droplets is represented by the blue (*RUNX1/BRWD*1) and orange (*SMAD4/TCF4*) columns, whereas the total number of drops generated are represented by the grey columns. There were only positive drops generated from the probes targeting genes on chromosome 21.
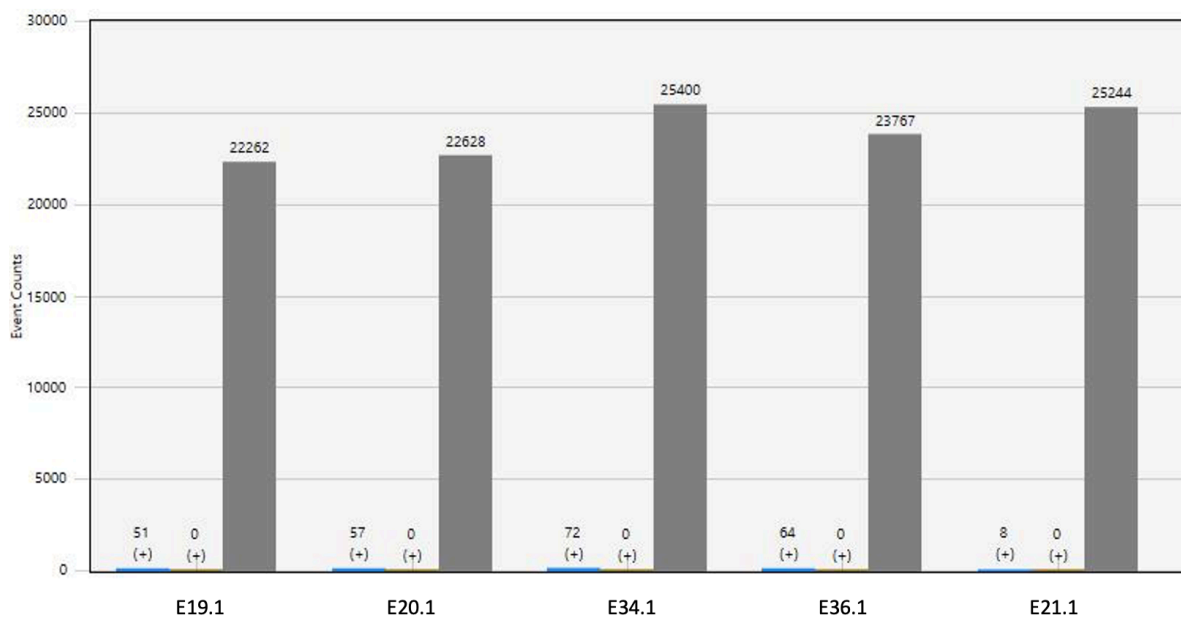
Figure 16 Overview of the merged droplets generated by digital droplet PCR (ddPCR) in five of the samples. *Both positive (+) from both probes (blue – RUNX1/BRWD1, yellow – SMAD4/TCF4) and the total number (grey – both positive and negative) of droplets generated in the duplicates are presented. No droplets were positive for the reference genes. Samples taken from the spent culture media (SCM) are represented by x.1, while samples taken of the whole dissociated blastocyst are represented by x.5.*
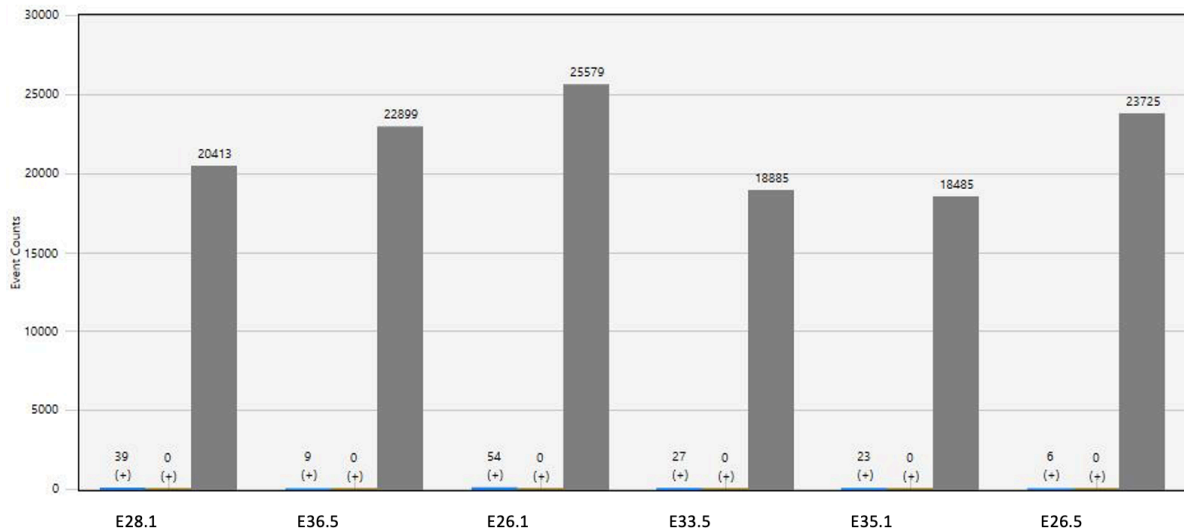
Figure 17 Overview of the merged droplets generated by digital droplet PCR (ddPCR) in six of the samples. *Both positive (+) from both probes (blue – RUNX1/BRWD1, yellow – SMAD4/TCF4) and the total number (grey – both positive and negative) of droplets generated in the duplicates are presented. No droplets were positive for the VIC probes, only the FAM probes. Samples taken from the spent culture media (SCM) are represented by x.1, while samples taken of the whole dissociated blastocyst are represented by x.5*

The starting concentration of the target molecule can then be determined in units of copies/µl by using a Poisson algorithm by fitting the fraction of positive droplets against the total number of droplets. The samples that had positive droplets detected had their starting concentration determined, which ranged from 0.599 copies/µl to 4.35 copies/µl. (Figure 18).
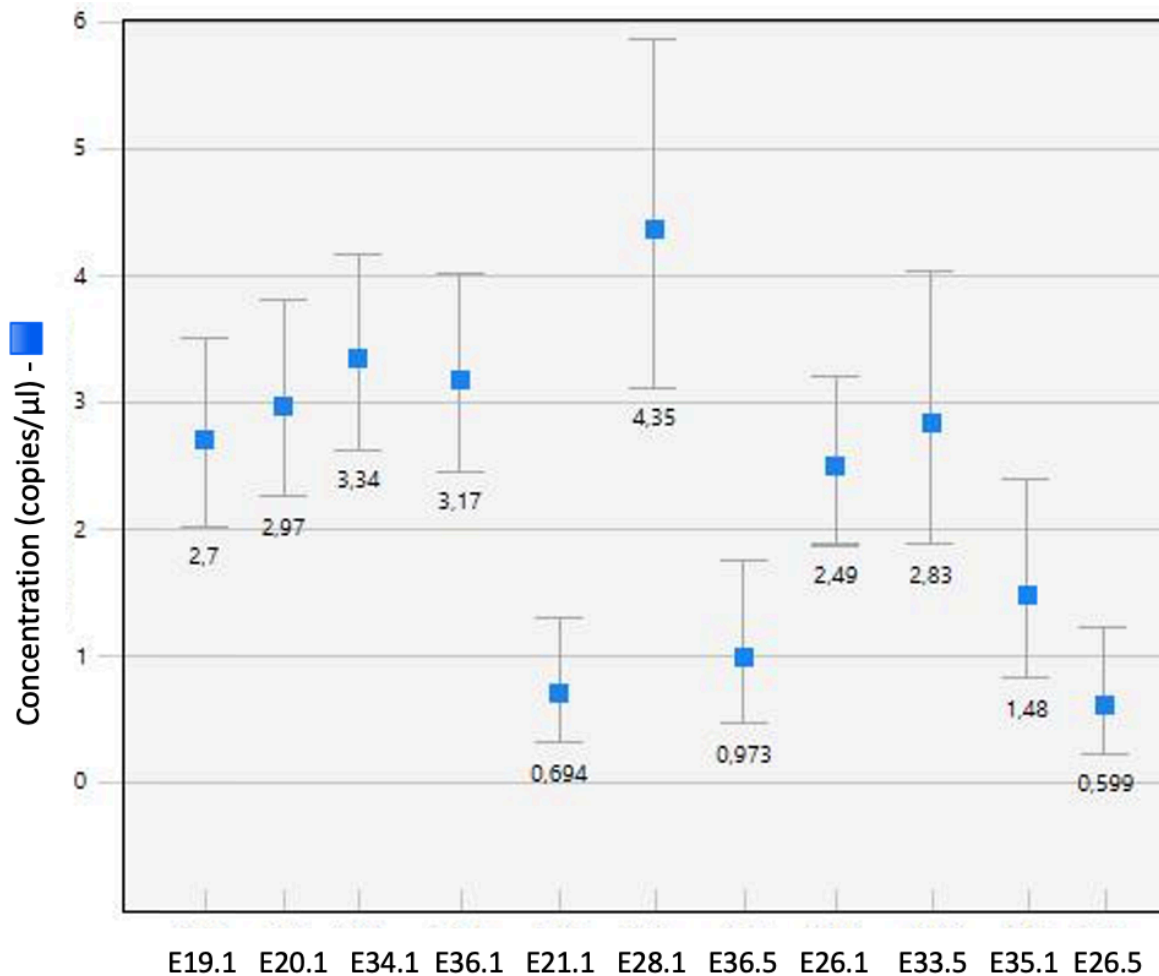
Figure 18 The concentration in unit copies/µl are presented for the samples obtaining positive droplets from the ddPCR run. The concentration is determined by fitting the fraction of positive droplets to a Poisson algorithm.

The only two samples which had positive droplets in both biopsies were embryos 26 and 36. They both have similar results with the concentration being higher in the SCM biopsy than in the whole blastocyst dissociation sample. Embryo 26 had a starting concentration of 2.49 copies/µl in the SCM biopsy, while the starting concentration in the whole blastocyst dissociation sample was 0.599 copies/µl. Embryo 36 had a starting concentration of 3.17 copies/µl in the SCM biopsy, while the starting concentration in the whole blastocyst dissociation sample was 0.973 copies/µl. Interestingly, this trend was similar for the other samples, with the majority of samples being collected from the SCM having a higher concentration than the samples collected from the whole blastocyst biopsies. Only diverging from this trend was sample E21.1, which was lower than 1 copies/µl, and E33.5, which was higher than 2 copies/µl. However, these remaining samples have no sample from the opposite biopsy to confirm that there seems to be a higher starting concentration in the SCM biopsies

than in the whole blastocyst biopsies. Further investigation is, therefore, necessary to see whether this trend is supported by more evidence or not.

Moreover, as there were no reference genes detected to determine how the concentrations of the genes located on chromosome 21 compared to those located on chromosome 18, these concentrations are not put into a complete picture. Interpretation of these concentrations should, therefore, not result in anything other than the fact that it is possible to detect genes involved in trisomy 21 from both biopsies. Additionally, it is noteworthy that multiplexing of the probes was not permitted in the software version used when ddPCR was performed, and the droplets that were positive for the FAM channel are a merged result from both genes targeted by the two probes: *BRWD1* and *RUNX1*. It is, thus, not possible to distinguish which genes were detected and resulted in the positive droplets, only that there were positive droplets generated from either or both probes in the sample.

5 Discussion

5.1 Storage, Quantitation and Amplification

Over the course of this study, 36 embryos in total were thawed. The first seven embryos were used to acquire the necessary skills to handle, culture, and dissociate the embryos, whereas the remaining 29 embryos were used in the downstream analysis. During the thawing process it was observed that the embryos frozen on day 3 were of inferior quality than those frozen on day 5. The day 3 embryos had a higher amount of fragmentation already present in the embryos after thawing, resulting in these being terminated within the first 48 hours of incubation, compared to the day 5 embryos. This could be explained by outdated protocols for cryopreservation, affecting the quality and viability of embryos after long-term storage.

The embryos used in this study was stored in a biobank that has been stored for more than ten years. The protocols used to freeze the embryos, the media used to culture them, and the criteria used to assess the embryos have progressed over the years. This implicates that the embryos that were stored over ten years ago may not fulfil today's criteria. Furthermore, the anonymization of the embryos, the lack of records for when they were stored, or what grade they were given at that time, may result in embryos of various quality being thawed. Therefore, their true state is only revealed once the thawing is complete. This may explain the higher fragmentation observed in the day 3 embryos thawed during the study, which might not be a true representation of the normal developing embryo as they could have been affected by

outdated protocols, grading schemes, and medias. Yet, the quality in the remaining embryos used in this study were good, indicating good viability despite the long-term storage. This is especially the case for the day 5 embryos, which had a less fragmentation overall. Fragmentation is a dynamic process where the fragments may be incorporated back into the cells by resorption, lysis, or internalization (115-117). However, a higher degree of fragmentation is associated with a reduced likelihood of the embryo implanting and, thus, no pregnancy (117, 118), outlining the importance of good viability in the embryos despite the long-term storage.

Dissociation of the embryos was performed even on the fragmented and terminated embryos, where the zona pellucida was punctured by repeated resuspension in the media and the cells were consequently released. Once the cells have left the zone pellucida, they are left undistinguishable from each other (i.e., TE cells are undistinguishable from the ICM cells), and they are dissociated into either single cells or clusters of cells. Four embryos (embryos 6, 9, 14, and 27) did not successfully dissociate, which could have impacted the amount of DNA extracted and isolated from these biopsies in downstream analysis.

To remove the possibility of getting any residue or particles from the SCM to affect the downstream analysis, both biopsy samples were treated with the MinElute Media Kit to extract and purify the DNA. Taking a closer look into other studies investigating the cfDNA from embryo cultures (12, 98-102, 119), there was only one study that specified that both their samples (i.e., SCM and whole blastocyst) were lysed before amplification was performed (104). Despite this, to prove that cfDNA was able to be detected and identified with the downstream applications, an extraction kit was opted for both samples during this study.

Given the nature of the embryo biopsy samples, it was expected that there would be little DNA present, if any, especially in the SCM biopsy samples containing only cfDNA. Therefore, to best establish what method would give the most reliable DNA quantitation of the isolated DNA, different methods were used; Qubit and NanoDrop. Quantitation by Qubit gave concentrations ranging from 0.23 ng/μl to 8.26 ng/μl, whereas the couple of samples that were quantitated using NanoDrop gave concentrations of 122.35 ng/μl and 193.05 ng/μl, which is considerably higher. In view of this gap between the methods and the knowledge of the small amount of DNA expected to be present in the samples, the most reliable option of quantitation for this study was chosen to be Qubit.

Quantitation by Qubit determined a mean concentration in the samples of 1.53 ng/µl, where the sample with the highest concentration was sample E31.5 with 8.26 ng/µl and the sample with the lowest concentration was sample E25.5 with 0.23 ng/µl. Sample E31.5 was taken from the whole blastocyst after dissociation, so a higher amount of DNA was expected, especially as the embryo was at the stage of expansion and hatching where the embryo can have up to 256 number of cells (106). Sample E25.5 was also taken as a dissociation sample; however, the embryo did not advance from the cleavage stage as a result of heavy fragmentation and there were, thus, less cells to make up the genetic material. Fragmentation is often associated with a range of factors (120), including advanced maternal age (121), chromosomal abnormalities (122), apoptosis (123) and oxidative stress (124), to mention a few. These factors may contribute to DNA damage and give a possible explanation for the low DNA concentration found in this particular sample, in addition to the low number of blastomeres.

The eight embryos with a higher concentration in their SCM sample compared to their whole blastocyst dissociation sample, embryos 8, 15, 25, 27, 29, 32, 34, and 36, could be explained by different reasons, such as contamination by either the semi-sterile lab-work environment or from maternal DNA (101), both being limitations of the study. It could also be explained by the embryo's failure to reach a new developmental stage or insufficient lysis of the cells during the extraction of DNA.

Investigation into different amplification methods was performed to choose the method with the best fit for this study. After a comparison of the most used kits for amplification of embryo-derived material in different studies based on effectiveness, time spent, and fit for the material of this study (125), the best fit was found to be Repli-G. Repli-G is a method based on MDA, which was found to be preferred due to the low-error rate of the ϕ29 DNA polymerase because of its endonuclease activity and its sufficient yield of DNA products, even with little starting material (12, 111). The specific kit that was used is also specifically made for samples with single cells or low DNA quantity, making it especially fitting for the purpose of this study. With the incredibly high fold increase in the samples after amplification, Repli-G proved to be a good fit.

Quantitation by NanoDrop determined a mean DNA concentration more than 200 times higher than the mean determined by Qubit for embryo 8. This is a value much higher than what is to be expected given the nature of the samples, giving reason to believe that quantitation by NanoDrop is unreliable for these kinds of samples. This might be explained by the instrument's

inability to distinguish between the nucleic acid or protein being tested (126) or interference of possible contaminants in the sample. Another study performed on cfDNA derived from malignant melanoma and prostate cancer patients also found that NanoDrop seemed less sensitive in the quantitation of samples with relatively low DNA concentrations, such as those with cfDNA, and concluded that quantitation by Qubit was more reliable with samples of such origin (127).

Even though NanoDrop was found to be less sensitive to the embryo-derived samples before amplification, NanoDrop was used to determine the purity and quality of the Repli-G amplified samples. The absorbance ratios were within the accepted range for all samples in both absorbance ratios 260/280 and 260/230, indicating pure DNA in the samples. The values determined for the amplified samples revealed over a thousandfold increase in concentration, clearly showing that amplification of the samples by Repli-G was successful. Yet, because NanoDrop did show some unreliable tendencies, quantitation was performed by Qubit to determine the concentration more accurately in the amplified samples. The samples were diluted 1:10 before quantitation by Qubit to make sure they were within the range of detection of the high sensitivity dsDNA assay kit. Quantitation then revealed relatively consistent values ranging from 60 ng/μl to 90 ng/μl in the samples, indicating good amplification by Repli-G.

5.2 Nanopore Sequencing

As briefly mentioned, only 5 embryos and their respective samples were amplified and used to perform nanopore sequencing. The embryos were chosen based on their DNA concentration, what developmental stage they had reached during the culturing, and whether their dissociation was successful or not. The five embryos chosen had concentrations above 0.5 ng/μl in their SCM samples and concentrations ranging from 0.8 ng/μl to 8 ng/μl in their whole blastocyst biopsy sample. Additionally, all the embryos reached the blastocyst stage ranging from being early blastocysts to hatching blastocyst, with all five being successfully dissociated. By choosing embryos that all were successfully dissociated and had a certain amount of DNA present, gave more promise to the amplification, which did show success by the large fold increase. Furthermore, by picking embryos that all have reached the blastocyst stage, illustrates how the method can be used in the future to investigate the health of blastocysts from individuals/couples undergoing IVF-treatment.

Before library preparation ensued, the samples were diluted with nuclease-free water to obtain the same concentration of 20.8 ng/μl in 48 μl, which correlates to the input amount of 1000 ng

DNA. It is expected that some DNA is lost during the clean-up, where the original input of 1000 ng reduces to roughly 400-500 ng after adaptor ligation and clean-up. The samples were quantitated after library preparation and barcoding was done, revealing concentrations ranging from 19 ng/μl to 26 ng/μl, showing consistent concentrations across the samples. Even with the expected loss of DNA in the samples from library preparation and barcoding, there was still enough DNA to produce a pooled sample of 800 ng (i.e., 80 ng from each sample) as input to perform sequencing. During the sequencing the nanopores were blocked, resulting in a shortened run as the pores were unable to capture and sequence another DNA molecule. To achieve a higher output of data, the flow cell was washed, and the samples were run again but with the same outcome, limiting the overall output from the sequencing runs.

A possible explanation for why the samples ended up blocking the pores during the sequencing could be the lack of a clean-up step after the amplification (128). Instead of being treated with a clean-up step or a T7 endonuclease treatment, the samples were put directly into storage at 4°C until library preparation ensued. This results in the hyperbranched structure that forms during amplification not being resolved and could also have resulted in possible residue or other contaminants from the amplification kit being present in the sample, disturbing the pores and, hence, blocking them once the DNA molecules were processed. In future experiments, a clean-up step should, therefore, be added to remove the possibility of contamination and see whether this affects the blocking and the output sequence data produced. Sequencing embryo-derived cfDNA has never been performed before on nanopore platforms and the protocols used to perform the sequencing in this study was, therefore, based on a study using liquid biopsies containing cfDNA from lung cancer patients (129). With more knowledge and better protocols issued for the samples of cfDNA-origin in the future, a better output may be generated.

The input DNA quality and quantity are also of importance, as too much or too little DNA or DNA of poor quality, such as heavily fragmented DNA, can affect the library preparations and, in return, the downstream sequencing as well. Cell-free fetal DNA (cffDNA) found in the maternal plasma used in prenatal testing is shed from the fetus and characterized by its fragmentation (130), suggesting that the cfDNA found in the SCM may have a degree of fragmentation as well. This demonstrates the importance of developing protocols that support fragmented DNA (i.e., cfDNA), having embryos of good quality without fragmentation, and choosing an amplification method that allows for successful amplification so that the necessary amount of DNA is available to perform sequencing.

As a result of the sequencing runs being cut short, there was not a sufficient number of reads generated for the different samples, which removes the possibility of getting a full picture on how the method can be applied to investigate the genetic state of embryos. However, there was still enough data produced to get a slight insight into how well the cfDNA was picked up in the SCM samples. It was expected that the mean read length should be longer for the whole blastocyst dissociation samples as these samples contains larger fragments of DNA, than those from the SCM containing cfDNA. Embryo 11 was the only embryo that had generated reads within the same region to produce an overlap correlation, but this is probably due to the limited number of reads generated from the sequencing. Improvements in the sequencing time is, therefore, necessary to see if overlap can be accomplished in the two sample biopsies with increased sequencing time and, thus, potentially the number of reads generated.

Furthermore, the blastn-search verified the consensus sequence generated, indicating that the data contains real DNA sequences. The consensus sequence was generated from the SCM biopsy sample of embryo 18, suggesting that the cfDNA found in the samples may be used to perform a genome-wide analysis of the embryo when more data is available. With improvements in the preparations of the samples, nanopore sequencing may represent a possible alternative to the investigation of the genomic state of the embryo used in IVF-treatments.

Over the course of this study, newer technology has been developed by the Oxford Nanopore Technology company. The introduction of short fragment mode, a new update installed on every software connected to a nanopore sequencer, allows for sequencing of DNA fragments down to 20 bp in length on nanopore platforms (131). This new update will make it even easier to detect and sequence fragments originating from cfDNA, without removing its sequencing ability of longer fragments, which results in a larger sequencing output being generated. Additionally, Remora the latest methylation tool developed by Oxford Nanopore Technology, allows easy access to the methylation information of short molecules, such as cfDNA (131). DNA methylation is involved in regulation of gene expression (132), and accessing that sort of information might give a further insight into what genes are expressed during the embryonic development.

With these advancements in mind, in addition to the important advantage of sequencing-time, further investigation into the use of nanopore sequencing for genetic analysis of embryos should be performed. Not only would information on the embryos be available for whole chromosomal aneuploidies, but with a deeper sequence coverage, information on mosaicism and segmental

abnormalities would also be available. This would allow the analysis to be personalized and adjusted to meet the needs of the one receiving it, with deeper sequencing being optional. However, further investigation into the optimization of this method is needed to generate a better foundation for downstream analysis and application.

5.3 Digital Droplet PCR

Optimally, there should be produced between 10 000 and 20 000 droplets by ddPCR, where any less than a total of 10 000 droplets in a well could result in the loss of template and give false negatives or false positives. Six wells generated under 10 000 droplets out of the 38 wells ddPCR was performed on. During the transfer of the droplets from the cartridge to the ddPCR plate it is crucial to have the right equipment and the right technique to not squeeze the droplets, as it will affect the number of droplets that are read (133). Droplets can get squeezed either by having a too tight opening in the pipet tip or by holding the pipet at an angle that doesn't allow the droplets to freely pass from the pipet into the well. Nonetheless, if this were the case for the samples on this run, it would be hard to explain why samples that were transferred simultaneously did not get squeezed by either the pipet tip or by having the wrong angle while pipetting. However, as false positives or false negatives could be detrimental in this type of research, practice is necessary to exclude technique from the possibilities of generating a low droplet count in the future.

Another possible explanation could be that the total volume of droplets generated was not transferred, giving a lower count than what was originally generated. Additionally, when mixing the reagents, the concentrations of both the supermix and the probes in the final mixture are crucial to produce enough droplets (133). By inaccurate measurement or pipette technique, some of the reagents could be lost, resulting in the wrong concentration in the mixture. This could explain why some samples had fewer droplets generated than others. Ideally, the run should have been performed again to make sure that the total droplet count was above the 10 000-droplet threshold in all samples.

The samples containing positive droplets detected for the genes located on chromosome 21, *BRWD1* and *RUNX1*, show how ddPCR can be used to detect genes involved in trisomy 21, even in samples originating from cfDNA found in the SCM of the embryos. However, only three out of the nine embryos analyzed had positive droplets generated for their whole blastocyst dissociation sample, which is concerning. These samples should contain the entire genome and should have had at least a baseline of droplets detected for the genes located on

chromosome 21. Furthermore, the lack of detection from any of the two probes in the VIC channel targeting the genes *TCF4* and *SMAD4* located on chromosome 18, removes the possibility of having a reference for comparison of the positive droplets. This leaves the data unreliable and even though the detection of the trisomy 21 genes in the cfDNA samples is promising, it is still necessary to do further investigation into this method and the probes used to see whether it can be optimized for the purpose of niPGT-A.

There was initially no gradient PCR performed to determine the optimal annealing temperature in the four probes used in ddPCR, as the probes had been validated by a published paper using these assays for detection of trisomy 21 in prenatal testing of cffDNA found in the maternal circulation (114). However, as the lack of signal of either probe targeting the reference genes and the probes targeting the genes located on chromosome 21, a validation assay should be set up to see whether another temperature leads to improved annealing and, in turn, rule out any flaws within the assays, or if new assays should be reordered. It is worth mentioning that a fellow classmate also failed to get detection of their probes in the VIC-channel while performing ddPCR, and their assays were also from Thermo Fisher. New assays for the genes located on chromosome 18 have, thus, been ordered to see if the lack of detection was a result of manufactual error in the original assays used in this study.

While ddPCR needs more investigation before a conclusion can be drawn on its application to performing a genetic analysis on embryos, it would be beneficial to see whether there is potential or not. ddPCR is a relatively cheap and easy technique to perform, and if it could provide reliable results to the health of an embryo, it could easily be applied to the routine diagnostics of an IVF-lab. With that said, however, ddPCR is a target-specific amplification method and its use would, therefore, be limited to only detecting the genes that are targeted. Contrastingly, nanopore technology may provide a deeper coverage and can, accordingly, provide a greater genetic analysis to a bigger patient group than ddPCR. The investigation into ddPCR should continue, but as the clinical patient group is smaller, the investigation should know its limit if the potential seems to be missing after continued troubleshooting.

5.4 Study Limitations

The research was carried out in a semi-sterile environment, both the culturing of the embryos, but also the downstream analysis of the embryos. This can of course implicate the results of the study, as DNA from other sources may contaminate the samples. Normally, IVF procedures such as embryo culturing and analysis are performed in sterile laboratory environments when

patients are involved. This is to remove the possibility of contaminations or other errors to occur. However, as no patients were involved in this study and the embryos were only used for research purposes, there was no setup available to carry out this study in a total sterile environment.

Another limitation is the lack of training in handling the embryos and biopsy-taking. Since the embryos are an invaluable and precious material, there were no embryos to spare for solely training purposes. Yet, the first seven embryos thawed were used to get to know the culturing of the embryos better, to learn how to dissociate them, and in the pre-runs of the different platforms used in downstream analysis. Normally, to become a certified clinical embryologist by the European Society of Human Reproduction and Embryology (ESHRE) standards, you need to have at least three years of experience (134), making the short amount of time available in which I worked with the embryos not sufficient to be fully trained. This needs to be taken into consideration, as the lack of training does pose a limitation to the quality of the work performed during this study. Other studies (i.e., where the embryo is the material of investigation) have used properly trained embryologists or IVF clinicians to perform the routine protocols involving the handling of the embryo's used in their research (12, 98-104, 119), which was not the case for this study.

There has been an ongoing discussion in the research community regarding the nature of the cfDNA in the SCM samples of embryos, whether it is a result of self-correcting mechanisms or if it is a contamination of maternal DNA. A study performed in 2018 combined chromosomal analysis of DNA collected from the SCM, follicular fluid, and embryonic DNA from the TE to reveal and identify maternal contamination in the samples (101). In accordance to previous findings (135), they found that the amount of cfDNA was greater for samples taken from the SCM that had been exposed to embryos compared to those that had not. They also found that even though it has been suggested that the cfDNA are secreted out from the embryo in conjunction with correction mechanisms for aneuploidies (135), that there were no significant differences in the amount of cfDNA in the media from aneuploid versus euploid embryos (101). However, they also found a significant amount of maternal DNA in all the samples analyzed by SNP array, and that the percentage of embryonic cfDNA found in the SCM samples ranged from 0% to 100% in the samples, suggesting that the embryonic genome might not be uniformly represented in the SCM of all embryos (101).

There was no investigation performed in this study to check whether maternal contamination could be a potential limitation, but based on previous findings, (101), one should take into consideration that it is a possibility. During the freezing and thawing process, the embryo is exposed to multiple washing steps that in theory should wash away any remnants of the cumulus oophorus cells (i.e., a cluster of cells surrounding the oocyte in the ovarian follicle (136)) that could give rise to a possible maternal DNA contamination. Nevertheless, based on previous findings further investigation should be performed to check whether the results obtained truly represent the embryo and that no source of contamination is present, either from the lab environment or from maternal DNA.

6 Social and Ethical Implications of the Study

There are several factors to consider when working with embryos, especially ethical ones, as the discussion of when human life begins is ever-present. Some would say that fertilization is the start of human life, while others would say such a notion is incorrect as a fertilized egg has no means to survive without an incubator before implantation. With the incubator being either in the form of a human uterine tube, a uterus, or a mechanical instrument. The distinction between when a human life starts and when cells that are alive fuse together and continue to live as an aggregation of stem cells, can sometimes get blurry between religious beliefs, politics, and ethics. It is, therefore, important to remember that the handling of embryos is not the same as the handling of human life. Embryos have the potential of producing a pregnancy that represents the possibility of new life being created, but an embryo is not considered a human life in itself.

Yet, the embryos do represent the possibility of new life and it is important to handle them as such. There are laws set in place to protect the possibility of life, to reduce the manipulation being performed before implantation, and to reduce permissibility of bias in choosing one's offspring. This is why the embryos should not be handled past day 14 after fertilization and why their use in research is limited to developing and improving methods and technology to achieve pregnancy. In other words, research performed on embryos in Norway is only allowed with the notion that the research should contribute to better knowledge and care for those in need of IVF or PGT-A.

Furthermore, as infertility and the inability to conceive children have become globally increasing problems, the need for solutions and better treatment has become necessary, not only

to accommodate today's needs, but to be prepared for the future problems and the increasing demand within the field. Alongside the increasing problem of infertility is the increased demand of treatment, and today's treatment are limited by several factors, such as cost, effectiveness, qualification, and time. IVF-treatments are highly expensive, not just for the couples or individuals undergoing them, but also for the society. Therefore, it is vital that we continue to investigate and develop better alternatives that can be more cost-effective and provide IVF as an alternative to more individuals and couples. This study aimed to investigate alternatives to the already existing treatments, which would be less expensive and reduce the time it takes for investigation into the embryonic genome. It would allow more couples to receive treatment as it becomes more available and the time to treat, hopefully, reduces as the treatment options improve. Non-invasive methods also mean less manipulation being performed on the embryo, which will also reduce the ethical complication surrounding IVF and the diagnostic routines performed.

7 Conclusion

In conclusion, long-term storage gave viable embryos, with day 5 embryos being of slightly better quality than those frozen on day 3. Both sampling approaches, SCM biopsy and dissociation, were successful where quantitation of both types of biopsies revealed presence of DNA in every sample collected. Qubit was found to be the most reliable option for quantitation of samples with a low concentration, such as those of cfDNA origin. Furthermore, amplification by Repli-G was found to be the most suitable amplification-method, which showed success with over a thousandfold increase in concentration of the samples. Investigation into nanopore sequencing revealed detection of cfDNA in all samples, but with limited output data generated, a genetic analysis could not to be performed. Additionally, ddPCR did get a detection of genes involved in trisomy 21, even in the cfDNA samples, but had a lack of detection for the reference genes. Further investigations into both methods for aneuploidy analysis of embryos is necessary before a conclusion can be drawn on the application of each method. Yet, the possibility of using cfDNA as an alternative to cell biopsies is promising and should continue to be explored.

8 Future Perspectives

Intending to develop better treatment for those in need of IVF, several factors should be improved to be able to provide this. Embryos used in future research should be stored with some sort of characterization of the morphology that reveals its quality before thawing, to allow the morphological assessment to be followed from before they are cryopreserved. This type of research should aim to be performed in a sterile environment, so that the technique may be applied diagnostically in the future. Furthermore, to remove the possibility of maternal contamination, haplotyping should be performed on both the maternal DNA and the embryo. This does add an extra step in the analysis but will produce even more reliable results and reveal how the embryonic genome is represented in the cfDNA and, therefore, its true application in the niPGT-A arena. Removing the possibility of maternal contamination also removes the possibility of having consequential error in downstream analysis, which is important as the aim is to provide an analysis that is of clinical relevance. An analysis may also be performed for both fresh and cryopreserved embryos, to compare and see whether there are any major differences in the amount of cfDNA that is secreted and if there may be a linkage between maternal contamination and the different protocols used. Another possibility

Improvements in the library preparations for nanopore sequencing that allows better retention of shorter fragments and a greater sequencing output, coupled with the subsequent use of short fragment mode may give a greater background for performing embryo analysis. Given that all pregnant women in Norway are receiving prenatal diagnostic analyses, it would be natural that the development of healthcare opts to offer and provide diagnostics to all individuals and couples undergoing IVF as well in the future. Personalized analysis may be possible to do with nanopore sequencing, as the sequencing run can be adjusted to meet the needs of the one receiving it (i.e., deeper coverage could be performed for those with hereditary diseases or cases with known segmental abnormalities). Futuristically, if cfDNA analyzed by nanopore sequencing proved to be a reliable source of information on the genetic state of the embryos, the handheld nanopore sequencer MinION could be equipped at the IVF-unit directly. This would allow for rapid analysis, and the possible exclusion of the freeze-thaw cycle could provide even faster treatment.

Furthermore, the introduction of new and improved technology regarding morphological assessment with the use of a time-lapse microscope allows the embryos to be assessed as a continuum with an image being captured every few minutes. This could more accurately

represent the highly dynamic preimplantation development period that the embryo goes through before transfer and may also allow for better grading as the grading is highly dependent on the time after insemination to reach a certain stage of development. Today, embryos are assessed at certain time points and the assessment is, therefore, more reliant on the time after insemination and not the natural development of the embryo itself. Embryos with aneuploid cells develop faster as they require a higher proliferative rate to make up for the apoptotic cells. Using a time-lapse microscope can, thus, be a possible way to evaluate the embryo being completely non-invasive, as the embryo is only morphologically assessed and not manipulated. However, this does not give an exact answer to the true state of the embryo and cannot replace a genetic analysis. In the future, a morphological assessment might be performed by an embryoscope paired with an SCM biopsy, which could be taken while the embryo is still in the incubator. Another advantage is that molecules such as RNA and metabolites that are present in the SCM as well could be analyzed to give a better understanding of the status of the embryo, and thus, aid in choosing the right embryo for transfer. The combination of the embryoscope and SCM biopsy may be the preferred method in the future to get the truest representation of the state of the embryo and its full implantation potential.

References

1.   The European Society for Human Reproduction and Embryology (ESHRE), Fertility Europe, Merck KGaA. A Policy Audit on Fertility - Analysis of 9 EU Countries. 2017.
2.   Brugo-Olmedo S, Chillik C, Kopelman S. Definition and causes of infertility. Reproductive BioMedicine Online. 2001;2(1):173-85.
3.   Mahalingaiah S, Hart JE, Laden F, Farland LV, Hewlett MM, Chavarro J, et al. Adult air pollution exposure and risk of infertility in the Nurses' Health Study II. Human Reproduction. 2016;31(3):638-47.
4.   Lal A, Roudebush WE, Chosed RJ. Embryo Biopsy Can Offer More Information Than Just Ploidy Status. Frontiers in Cell and Developmental Biology. 2020;8(78).
5.   Banker M, Dyer S, Chambers GM, Ishihara O, Kupka M, de Mouzon J, et al. International Committee for Monitoring Assisted Reproductive Technologies (ICMART): world report on assisted reproductive technologies, 2013. Fertility and Sterility. 2021:1588-609.
6.   Fragouli E, Lenzi M, Ross R, Katz-Jaffe M, Schoolcraft WB, Wells D. Comprehensive molecular cytogenetic analysis of the human blastocyst stage. Human Reproduction. 2008;23(11):2596-608.
7.   Kushnir VA, Frattarelli JL. Aneuploidy in abortuses following IVF and ICSI. Journal of Assisted Reproduction and Genetics. 2009;26(2):93-7.
8.   Fragouli E, Wells D. Aneuploidy in the Human Blastocyst. Cytogenetic and Genome Research. 2011;133(2-4):149-59.
9.   De Sutter P, Stadhouders R, Dutré M, Gerris J, Dhont M. Prevalence of chromosomal abnormalities and timing of karyotype analysis in patients with recurrent implantation failure (RIF) following assisted reproduction. Facts, Views & Vision in Obstetrics and Gynaecology. 2012;4(1):59-65.
10.   Sandalinas M, Sadowy S, Alikani M, Calderon G, Cohen J, Munne S. Developmental ability of chromosomally abnormal human embryos to develop to the blastocyst stage. Human Reproduction 2001;16(9):1954-8.
11.   Rubio C, Rodrigo L, Simón C. Preimplantation genetic testing: Chromosome abnormalities in human embryos. Reproduction. 2020;160(5):A33-A44.
12.   Shamonki MI, Jin H, Haimowitz Z, Liu L. Proof of concept: preimplantation genetic screening without embryo biopsy through analysis of cell-free DNA in spent embryo culture media. Fertility and Sterility. 2016;106(6):1312-8.
13.   Ambartsumyan G, Clark AT. Aneuploidy and early human embryo development. Human Molecular Genetics. 2008;17(R1):R10-R5.
14.   Moore KL, Persaud TVN, Torchia MG. First Week of Human Development. The Developing Human: Clinically Oriented Embryology. 9th ed. Canada: Elsevier Saunders; 2013. p. 13-40.
15.   Sadler TW. First Week of Development: Ovulation to Implantation. In: Wilkins LW, editor. Langman's Medical Embryology. 12th ed. USA: Wolters Kluwer Health, Lippincott Williams & Wilkins; 2012. p. 29-42.
16.   Dudek RW. Week 1 (Days 1-7). In: Wilkins LW, editor. High-Yield Embryology. 4th ed: Wolters Kluwer Health, Lippincott Williams & Wilkins; 2010. p. 7-11.
17.   Vázquez-Diez C, FitzHarris G. Causes and consequences of chromosome segregation error in preimplantation embryos. Reproduction. 2018;155(1):R63-R76.
18.   Carlson BM. Cleavage and Implantation. Human Embryology & Developmental Biology. 6th ed: Elsevier 2019. p. 52-70.

19.   Roux C, Joanne C, Agnani G, Fromm M, Clavequin MC, Bresson JL. Morphometric parameters of living human in-vitro fertilization embryos; importance of the asynchronous division process. Human Reproduction 1995;10(5):1201-7.

20.   Webster S, de Wreede R. Early Development. Embryology at a Glance. Oxford, England: John Wiley & Sons, Ltd.; 2012. p. 26-31.

21.   Dale B, Elder K. First Stages of Development. In-Vitro Fertilization. 4th ed. Cambridge: Cambridge University Press; 2020. p. 97-119.

22.   Carlson BM. Transport of Gametes and Fertilization. Human Embryology & Developmental Biology. 6th ed: Elsevier; 2019. p. 23-34.

23.   Rock J, Menkin MF. In Vitro Fertilization and Cleavage of Human Ovarian Eggs. Science. 1944;100(2588):105-7.

24.   Menkin MF, Rock J. In Vitro Fertilization and Cleavage of Human Ovarian Eggs. American Journal of Obstetrics and Gynecology. 1948;55(3):440-52.

25.   Shettles LB. A Morula Stage of Human Ovum Developed in Vitro. Fertility and Sterility. 1955;6(4):287-9.

26.   Steptoe PC, Edwards RG. Birth After the Reimplantation of a Human Embryo. The Lancet. 1978;312(8085):366.

27.   The Nobel Assembly at Karolinska Institutet. The Nobel Prize in Physiology or Medicine 2010 [Press Release]. Nobelprize.org: The Nobel Assembly at Karolinska Institutet; 2010 [10.10.21]. Available from: https://www.nobelprize.org/prizes/medicine/2010/summary/.

28.   Adamson GD, editor International Committee for Monitoring ART (ICMART). 34th annual Meeting of the European Society of Human Reproduction and Embryology; 2018; Barcelona, Spain.

29.   Edwards R, Patrizio P, Edgar D, Field C, Brinton L. Defining IVF terminology. Reproductive BioMedicine Online. 2007;14(5):553-4.

30.   Barton SE, Politch JA, Benson CB, Ginsburg ES, Gargiulo AR. Transabdominal follicular aspiration for oocyte retrieval in patients with ovaries inaccessible by transvaginal ultrasound. Fertility and Sterility. 2011;95(5):1773-6.

31.   Palermo G, Joris H, Devroey P, Van Steirteghem AC. Pregnancies after intracytoplasmic injection of single spermatozoon into an oocyte. The Lancet. 1992;340(8810):17-8.

32.   Viotti M. Preimplantation Genetic Testing for Chromosomal Abnormalities: Aneuploidy, Mosaicism, and Structural Rearrangements. Genes (Basel). 2020;11(6):602-38.

33.   Nussbaum R, McInnes R, Willard H. Glossary. Thompson&Thompson; Genetics in Medicine. 8th ed: Elsevier; 2016. p. 489-94.

34.   Nussbaum R, McInnes R, Willard H. Principles of Clinical Cytogenesis and Genome Analysis. Thompson&Thompson; Genetics in Medicine. 8th ed: Elsevier; 2016. p. 57-74.

35.   Verlinsky Y, Cieslak J, Ivakhnenko V, Evsikov S, Wolf G, White M, et al. Preimplantation diagnosis of common aneuploidies by the first- and second-polar body FISH analysis. Journal of Assisted Reproduction and Genetics 1998;15(5):285-9.

36.   Kuliev A, Verlinsky Y. Meiotic and mitotic nondisjunction: lessons from preimplantation genetic diagnosis. Human Reproduction Update. 2004;10(5):401-7.

37.   Nagaoka SI, Hassold TJ, Hunt PA. Human aneuploidy: mechanisms and new insights into an age-old problem. Nature Reviews Genetics. 2012;13(7):493-504.

38.   Hunt PA, Hassold TJ. Sex Matters in Meiosis. Science. 2002;296(5576):2181-3.

39.   Kubicek D, Hornak M, Horak J, Navratil R, Tauwinklova G, Rubes J, et al. Incidence and origin of meiotic whole and segmental chromosomal aneuploidies detected by karyomapping. Reproductive BioMedicine Online. 2019;38(3):330-9.

40.   Hassold T, Hunt P. To err (meiotically) is human: the genesis of human aneuploidy. Nature Reviews Genetics. 2001;2(4):280-91.

41.   Chiang T, Schultz RM, Lampson MA. Meiotic Origins of Maternal Age-Related Aneuploidy. Biology of Reproduction. 2012;86(1):1-7.

42.   Konstantinidis M, Ravichandran K, Gunes Z, Prates R, Goodall NN, Roman B, et al. Aneuploidy and recombination in the human preimplantation embryo. Copy number variation analysis and genome-wide polymorphism genotyping. Reproductive BioMedicine Online. 2020;40(4):479-93.

43.   Demko ZP, Simon AL, McCoy RC, Petrov DA, Rabinowitz M. Effects of maternal age on euploidy rates in a large cohort of embryos analyzed with 24-chromosome single-nucleotide polymorphism–based preimplantation genetic screening. Fertility and Sterility. 2016;105(5):1307-13.

44.   Franasiak JM, Forman EJ, Hong KH, Werner MD, Upham KM, Treff NR, et al. The nature of aneuploidy with increasing age of the female partner: a review of 15,169 consecutive trophectoderm biopsies evaluated with comprehensive chromosomal screening. Fertility and Sterility. 2014;101(3):656-63.e1.

45.   Irani M, Canon C, Robles A, Maddy B, Gunnala V, Qin X, et al. No effect of ovarian stimulation and oocyte yield on euploidy and live birth rates: an analysis of 12 298 trophectoderm biopsies. Human Reproduction. 2020;35(5):1082-9.

46.   Carrasquillo RJ, Kohn TP, Cinnioglu C, Rubio C, Simon C, Ramasamy R, et al. Advanced paternal age does not affect embryo aneuploidy following blastocyst biopsy in egg donor cycles. Journal of Assisted Reproduction and Genetics. 2019;36(10):2039-45.

47.   Dviri M, Madjunkova S, Koziarz A, Antes R, Abramov R, Mashiach J, et al. Is there a correlation between paternal age and aneuploidy rate? An analysis of 3,118 embryos derived from young egg donors. Fertility and Sterility. 2020;114(2):293-300.

48.   Nussbaum R, McInnes R, Willard H. The Chromosomal and Genomic Basis of Disease: Disorders of the Autosomes and Sex Chromosomes. Thompson&Thompson; Genetics in Medicine. 8th ed: Elsevier; 2016. p. 75-106.

49.   Held K, Kerber S, Kaminsky E, Singh S, Goetz P, Seemanova E, et al. Mosaicism in 45, X Turner syndrome: does survival in early pregnancy depend on the presence of two sex chromosomes? Human Genetics. 1992;88(3):288-94.

50.   Gaulden ME. Maternal age effect: The enigma of Down syndrome and other trisomic conditions. Mutation Research/Reviews in Genetic Toxicology. 1992;296(1):69-88.

51.   Penrose LS. The relative effects of paternal and maternal age in mongolism. 1933. Journal of Genetics 2009;88(1):9-14.

52.   Savva GM, Walker K, Morris JK. The maternal age-specific live birth prevalence of trisomies 13 and 18 compared to trisomy 21 (Down syndrome). Prenatal Diagnosis 2010;30(1):57-64.

53.   Boyd PA, Loane M, Garne E, Khoshnood B, Dolk H, a Ewg. Sex chromosome trisomies in Europe: prevalence, prenatal detection and outcome of pregnancy. European Journal of Human Genetics. 2011;19(2):231-4.

54.   Ratcliffe S. Long term outcome in children of sex chromosome abnormalities. Archives of Disease in Childhood. 1999;80(2):192-5.

55.   Treff NR, Franasiak JM. Detection of segmental aneuploidy and mosaicism in the human preimplantation embryo: technical considerations and limitations. Fertility and Sterility. 2017;107(1):27-31.

56.   Babariya D, Fragouli E, Alfarawati S, Spath K, Wells D. The incidence and origin of segmental aneuploidy in human oocytes and preimplantation embryos. Human Reproduction. 2017;32(12):2549-60.

57.	Mehta A, Haber JE. Sources of DNA double-strand breaks and models of recombinational DNA repair. Cold Spring Harbor Perspectives in Biology. 2014;6(9):a016428 1-17.

58.	Nussbaum R, McInnes R, Willard H. Human Genetic Diversity: Mutation and Polymorphism. Thompson&Thompson; Genetics in Medicine. 8th ed: Elsevier; 2016. p. 43-56.

59.	NIH National Library of Medicine. Can changes in the structure of chromosomes affect health and development? [Informational pamphlet]. medlineplus.gov: NIH, National Library of Medicine; 2021 [28.10.21]. Available from: https://medlineplus.gov/genetics/understanding/mutationsanddisorders/structuralchanges/.

60.	Vera-Rodríguez M, Michel C-E, Mercader A, Bladon AJ, Rodrigo L, Kokocinski F, et al. Distribution patterns of segmental aneuploidies in human blastocysts identified by next-generation sequencing. Fertility and Sterility. 2016;105(4):1047-55.e2.

61.	Treff NR, Northrop LE, Kasabwala K, Su J, Levy B, Scott RT. Single nucleotide polymorphism microarray–based concurrent screening of 24-chromosome aneuploidy and unbalanced translocations in preimplantation human embryos. Fertility and Sterility. 2011;95(5):1606-12.e2.

62.	Kort DH, Chia G, Treff NR, Tanaka AJ, Xing T, Vensand LB, et al. Human embryos commonly form abnormal nuclei during development: a mechanism of DNA damage, embryonic aneuploidy, and developmental arrest. Human Reproduction. 2016;31(2):312-23.

63.	Girardi L, Serdarogullari M, Patassini C, Poli M, Fabiani M, Caroselli S, et al. Incidence, Origin, and Predictive Model for the Detection and Clinical Management of Segmental Aneuploidies in Human Embryos. American Journal of Human Genetics 2020;106(4):525-34.

64.	Escribà M-J, Vendrell X, Peinado V. Segmental aneuploidy in human blastocysts: a qualitative and quantitative overview. Reproductive Biology and Endocrinology. 2019;17(1):76-91.

65.	Rabinowitz M, Ryan A, Gemelos G, Hill M, Baner J, Cinnioglu C, et al. Origins and rates of aneuploidy in human blastomeres. Fertility and Sterility. 2012;97(2):395-401.

66.	Wells D, Delhanty JDA. Comprehensive chromosomal analysis of human preimplantation embryos using whole genome amplification and single cell comparative genomic hybridization. Molecular Human Reproduction. 2000;6(11):1055-62.

67.	Cuman C, Beyer CE, Brodie D, Fullston T, Lin JI, Willats E, et al. Defining the limits of detection for chromosome rearrangements in the preimplantation embryo using next generation sequencing. Human Reproduction. 2018;33(8):1566-76.

68.	McCoy RC. Mosaicism in Preimplantation Human Embryos: When Chromosomal Abnormalities Are the Norm. Trends in Genetics 2017;33(7):448-63.

69.	Nussbaum R, McInnes R, Willard H. Patterns of Single-Gene Inheritance. Thompson&Thompson; Genetics in Medicine. 8th ed: Elsevier; 2016. p. 107-32.

70.	Munne S, Weier HU, Grifo J, Cohen J. Chromosome Mosaicism in Human Embryos. Biology of Reproduction. 1994;51(3):373-9.

71.	Taylor TH, Gitlin SA, Patrick JL, Crain JL, Wilson JM, Griffin DK. The origin, mechanisms, incidence and clinical consequences of chromosomal mosaicism in humans. Human Reproduction Update. 2014;20(4):571-81.

72.	Palermo G, Munne S, Cohen J. The human zygote inherits its mitotic potential from the male gamete. Human Reproduction. 1994;9(7):1220-5.

73.	Palermo GD, Colombero LT, Rosenwaks Z. The human sperm centrosome is responsible for normal syngamy and early embryonic development. Reviews of Reproduction. 1997;2:19-27.

74.   Terada Y, Nakamura Si, Simerly C, Hewitson L, Murakami T, Yaegashi N, et al. Centrosomal function assessment in human sperm using heterologous ICSI with rabbit eggs: a new male factor infertility assay. Molecular Reproduction and Development: Incorporating Gamete Research. 2004;67(3):360-5.

75.   Yoshimoto-Kakoi T, Terada Y, Tachibana M, Murakami T, Yaegashi N, Okamura K. Assessing centrosomal function of infertile males using heterologous ICSI. Systems Biology in Reproductive Medicine. 2008;54(3):135-42.

76.   Conlin LK, Thiel BD, Bonnemann CG, Medne L, Ernst LM, Zackai EH, et al. Mechanisms of mosaicism, chimerism and uniparental disomy identified by single nucleotide polymorphism array analysis. Human Molecular Genetics. 2010;19(7):1263-75.

77.   Sachdev NM, Maxwell SM, Besser AG, Grifo JA. Diagnosis and clinical management of embryonic mosaicism. Fertility and Sterility 2017;107(1):6-11.

78.   Gardner DK, Balaban B. Assessment of human embryo development using morphological criteria in an era of time-lapse, algorithms and 'OMICS': is looking good still important? Molecular Human Reproduction. 2016;22(10):704-18.

79.   Alpha Scientists in Reproductive Medicine Eshre Special Interest Group of Embryology. The Istanbul consensus workshop on embryo assessment: proceedings of an expert meeting. Human Reproduction. 2011;26(6):1270-83.

80.   Kort J, Behr B. Traditional Embryo Morphology Evaluation: From the Zygote to the Blastocyst Stage. In: Nagy ZP, Varghese AC, Agarwal A, editors. In Vitro Fertilization: A Textbook of Current and Emerging Methods and Devices. Cham: Springer International Publishing; 2019. p. 493-504.

81.   Gardner DK, Schoolcraft WB. Culture and transfer of human blastocysts. Current Opinion in Obstetrics and Gynecology. 1999;11(3).

82.   Poli M, Girardi L, Fabiani M, Moretto M, Romanelli V, Patassini C, et al. Past, Present, and Future Strategies for Enhanced Assessment of Embryo's Genome and Reproductive Competence in Women of Advanced Reproductive Age. Frontiers in Endocrinology 2019;10:154.

83.   Vermeesch JR, Voet T, Devriendt K. Prenatal and pre-implantation genetic diagnosis. Nature Reviews Genetics. 2016;17(10):643-56.

84.   Capalbo A, Ubaldi FM, Cimadomo D, Maggiulli R, Patassini C, Dusi L, et al. Consistent and reproducible outcomes of blastocyst biopsy and aneuploidy screening across different biopsy practitioners: a multicentre study involving 2586 embryo biopsies. Human Reproduction. 2016;31(1):199-208.

85.   Philip J, Bryndorf T, Christensen B. Prenatal aneuploidy detection in interphase cells by fluorescence in situ hybridization (Fish). Prenatal Diagnosis. 1994;14(13):1203-15.

86.   Harper JC, Wilton L, Traeger-Synodinos J, Goossens V, Moutou C, SenGupta SB, et al. The ESHRE PGD Consortium: 10 years of data collection. Human Reproduction Update. 2012;18(3):234-47.

87.   Treff NR, Levy B, Su J, Northrop LE, Tao X, Scott RT, Jr. SNP microarray-based 24 chromosome aneuploidy screening is significantly more consistent than FISH. Molecular Human Reproduction. 2010;16(8):583-9.

88.   Cooper ML, Darilek S, Wun WS, Angus SC, Mensing DE, Pursley AN, et al. A retrospective study of preimplantation embryos diagnosed with monosomy by fluorescence in situ hybridization (FISH). Cytogenetic and Genome Research. 2006;114(3-4):359-66.

89.   Li M, DeUgarte CM, Surrey M, Danzer H, DeCherney A, Hill DL. Fluorescence in situ hybridization reanalysis of day-6 human blastocysts diagnosed with aneuploidy on day 3. Fertility and Sterility. 2005;84(5):1395-400.

90.	Treff NR, Scott RT. Four-hour quantitative real-time polymerase chain reaction–based comprehensive chromosome screening and accumulating evidence of accuracy, safety, predictive value, and clinical efficacy. Fertility and Sterility. 2013;99(4):1049-53.

91.	Capalbo A, Treff NR, Cimadomo D, Tao X, Upham K, Ubaldi FM, et al. Comparison of array comparative genomic hybridization and quantitative real-time PCR-based aneuploidy screening of blastocyst biopsies. European Journal of Human Genetics. 2015;23(7):901-6.

92.	Fragouli E, Alfarawati S, Spath K, Babariya D, Tarozzi N, Borini A, et al. Analysis of implantation and ongoing pregnancy rates following the transfer of mosaic diploid–aneuploid blastocysts. Human Genetics. 2017;136(7):805-19.

93.	Munné S, Wells D. Detection of mosaicism at blastocyst stage with the use of high-resolution next-generation sequencing. Fertility and Sterility. 2017;107(5):1085-91.

94.	Kung A, Munné S, Bankowski B, Coates A, Wells D. Validation of next-generation sequencing for comprehensive chromosome screening of embryos. Reproductive BioMedicine Online. 2015;31(6):760-9.

95.	Wei S, Weiss ZR, Gaur P, Forman E, Williams Z. Rapid preimplantation genetic screening using a handheld, nanopore-based DNA sequencer. Fertility and Sterility. 2018;110(5):910-6.e2.

96.	Jain M, Olsen HE, Paten B, Akeson M. The Oxford Nanopore MinION: delivery of nanopore sequencing to the genomics community. Genome Biology. 2016;17(1):239-50.

97.	Palini S, Galluzzi L, De Stefani S, Bianchi M, Wells D, Magnani M, et al. Genomic DNA in human blastocoele fluid. Reproductive BioMedicine Online. 2013;26(6):603-10.

98.	Xu J, Fang R, Chen L, Chen D, Xiao J-P, Yang W, et al. Noninvasive chromosome screening of human embryos by genome sequencing of embryo culture medium for in vitro fertilization. Proceedings of the National Academy of Sciences. 2016;113(42):11907.

99.	Gianaroli L, Magli MC, Pomante A, Crivello AM, Cafueri G, Valerio M, et al. Blastocentesis: a source of DNA for preimplantation genetic testing. Results from a pilot study. Fertility and Sterility. 2014;102(6):1692-9.e6.

100.	Ho JR, Arrach N, Rhodes-Long K, Ahmady A, Ingles S, Chung K, et al. Pushing the limits of detection: investigation of cell-free DNA for aneuploidy screening in embryos. Fertility and Sterility. 2018;110(3):467-75.e2.

101.	Vera-Rodriguez M, Diez-Juan A, Jimenez-Almazan J, Martinez S, Navarro R, Peinado V, et al. Origin and composition of cell-free DNA in spent medium from human embryo culture during preimplantation development. Human Reproduction. 2018;33(4):745-56.

102.	Yeung QSY, Zhang YX, Chung JPW, Lui WT, Kwok YKY, Gui B, et al. A prospective study of non-invasive preimplantation genetic testing for aneuploidies (NiPGT-A) using next-generation sequencing (NGS) on spent culture media (SCM). Journal of Assisted Reproduction and Genetics. 2019;36(8):1609-21.

103.	Rubio C, Navarro-Sánchez L, García-Pascual CM, Ocali O, Cimadomo D, Venier W, et al. Multicenter prospective study of concordance between embryonic cell-free DNA and trophectoderm biopsies from 1301 human blastocysts. American Journal of Obstetrics and Gynecology. 2020;223(5):751.e1-.e13.

104.	Huang L, Bogale B, Tang Y, Lu S, Xie XS, Racowsky C. Noninvasive preimplantation genetic testing for aneuploidy in spent medium may be more reliable than trophectoderm biopsy. Proceedings of the National Academy of Sciences. 2019;116(28):14105-12.

105.	Cooper Surgical Inc. Embryo Culture Guide [Guide]. coopersurgical.marketport.net2021 [01.04.22]. Available from: https://coopersurgical.marketport.net/MarketingZone/MZDirect/Source/bc783b50-708f-4e0b-ac94-f456c2db9440.

106.   Niakan K. Placental Biology Course. https://www.cambridge-africa.cam.ac.uk/cambridge-africa-updates/online-placental-biology-course-2021/: University of Cambridge; 5th-9th july 2021.

107.   Thermo Fisher Scientific. Qubit dsDNA HS Assay Kits [User Guide]. assets.thermofisher.com [updated 05.03.2015 cited 06.02.22]. Available from: https://assets.thermofisher.com/TFS-Assets/LSG/manuals/Qubit_dsDNA_HS_Assay_UG.pdf.

108.   Thermo Fischer Scientific. Nucleic Acid, Thermo Scientific NanoDrop Spectrophotometers [Technical Guide]. tools.thermofisher.com 2010 [updated November 2010 cited 06.02.22]. Available from: https://tools.thermofisher.com/content/sfs/brochures/Thermo-Scientific-NanoDrop-Products-Nucleic-Acid-Technical-Guide-EN.pdf.

109.   Matlock B. Assessment of Nucleic Acid Purity [Technical Note]. Thermo Fisher Scientific Thermo Fischer Scientific 2015 [01.06.2020]. Available from: https://assets.thermofisher.com/TFS-Assets/CAD/Product-Bulletins/TN52646-E-0215M-NucleicAcid.pdf.

110.   Dean FB, Hosono S, Fang L, Wu X, Faruqi AF, Bray-Ward P, et al. Comprehensive human genome amplification using multiple displacement amplification. Proceedings of the National Academy of Sciences. 2002;99(8):5261.

111.   Spits C, Le Caignec C, De Rycke M, Van Haute L, Van Steirteghem A, Liebaers I, et al. Whole-genome multiple displacement amplification from single cells. Nature Protocols 2006;1(4):1965-70.

112.   Dean FB, Nelson JR, Giesler TL, Lasken RS. Rapid amplification of plasmid and phage DNA using Phi 29 DNA polymerase and multiply-primed rolling circle amplification. Genome Research 2001;11(6):1095-9.

113.   Hindson BJ, Ness KD, Masquelier DA, Belgrader P, Heredia NJ, Makarewicz AJ, et al. High-Throughput Droplet Digital PCR System for Absolute Quantitation of DNA Copy Number. Analytical Chemistry. 2011;83(22):8604-10.

114.   El Khattabi LA, Rouillac-Le Sciellour C, Le Tessier D, Luscan A, Coustier A, Porcher R, et al. Could Digital PCR Be an Alternative as a Non-Invasive Prenatal Test for Trisomy 21: A Proof of Concept Study. PLoS One. 2016;11(5):e0155009.

115.   Van Blerkom J, Davis P, Alexander S. A microscopic and biochemical study of fragmentation phenotypes in stage-appropriate human embryos. Human Reproduction. 2001;16(4):719-29.

116.   Hardarson T, Löfman C, Coull G, Sjögren A, Hamberger L, Edwards RG. Internalization of cellular fragments in a human embryo: time-lapse recordings. Reproductive BioMedicine Online. 2002;5(1):36-8.

117.   Fujimoto VY, Browne RW, Bloom MS, Sakkas D, Alikani M. Pathogenesis, developmental consequences, and clinical correlations of human embryo fragmentation. Fertility and Sterility. 2011;95(4):1197-204.

118.   Staessen C, Nagy ZP, Liu J, Janssenswillen C, Camus M, Devroey P, et al. One year's experience with elective transfer of two good quality embryos in the human in-vitro fertilization and intracytoplasmic sperm injection programmes. Human Reproduction. 1995;10(12):3305-12.

119.   Rubio C, Bellver J, Rodrigo L, Bosch E, Mercader A, Vidal C, et al. Preimplantation genetic screening using fluorescence in situ hybridization in patients with repetitive implantation failure and advanced maternal age: two randomized trials. Fertility and Sterility. 2013;99(5):1400-7.

120.   Kim S-G, Kim Y-Y, Park J-Y, Kwak S-J, Yoo C-S, Park I-H, et al. Early fragment removal on in vitro fertilization day 2 significantly improves the subsequent development and

clinical outcomes of fragmented human embryos. Clinical and Experimental Reproductive Medicine 2018;45(3):122-8.

121.   Keltz MD, Skorupski JC, Bradley K, Stein D. Predictors of embryo fragmentation and outcome after fragment removal in in vitro fertilization. Fertility and Sterility. 2006;86(2):321-4.

122.   Phan V, Littman E, Harris D, La A. Correlation between embryo morphology and development and chromosomal complement. Asian Pacific Journal of Reproduction. 2014;3(2):85-9.

123.   Jurisicova A, Varmuza S, Casper RF. Programmed cell death and human embryo fragmentation. Molecular Human Reproduction. 1996;2(2):93-8.

124.   Otasevic V, Surlan L, Vucetic M, Tulic I, Buzadzic B, Stancic A, et al. Expression patterns of mitochondrial OXPHOS components, mitofusin 1 and dynamin-related protein 1 are associated with human embryo fragmentation. Reproduction, Fertility and Development. 2016;28(3):319-27.

125.   Brouillet S, Martinez G, Coutton C, Hamamah S. Is cell-free DNA in spent embryo culture medium an alternative to embryo biopsy for preimplantation genetic testing? A systematic review. Reproductive BioMedicine Online. 2020;40(6):779-96.

126.   Invitrogen. Comparison of fluorescence-based quantitation with UV absorbance measurements [Technical note]. tools.thermofisher.com: Thermo Fisher Scientific; 2016 [06.02.22]. Available from:
https://tools.thermofisher.com/content/sfs/brochures/fluorescence-UV-quantitation-comparison-tech-note.pdf.

127.   Ponti G, Maccaferri M, Manfredini M, Kaleci S, Mandrioli M, Pellacani G, et al. The value of fluorimetry (Qubit) and spectrophotometry (NanoDrop) in the quantification of cell-free DNA (cfDNA) in malignant melanoma and prostate cancer patients. Clinica Chimica Acta. 2018;479:14-9.

128.   Oxford Nanopore Technologies. Premium whole genome apmlification protocol (SQK-LSK109). version: WAL_9070_v109_revQ_14Aug2019 ed: Oxford Nanopore Technologies; 2019.

129.   Martignano F, Munagala U, Crucitta S, Mingrino A, Semeraro R, Del Re M, et al. Nanopore sequencing from liquid biopsy: analysis of copy number variations from cell-free DNA of lung cancer patients. Molecular Cancer. 2021;20(1):32-8.

130.   Whale AS, Fernandez-Gonzalez A, Gutteridge A, Devonshire AS. Control Materials and Digital PCR Methods for Evaluation of Circulating Cell-Free DNA Extractions from Plasma. In: Karlin-Neumann G, Bizouarn F, editors. Digital PCR: Methods and Protocols. New York, NY: Springer New York; 2018. p. 45-65.

131.   Oxford Nanopore releases Short Fragment Mode: a new tool for real-time sequencing of short fragments of DNA [press release]. nanoporetech.com 23/03 2022.

132.   Moore LD, Le T, Fan G. DNA Methylation and Its Basic Function. Neuropsychopharmacology. 2013;38(1):23-38.

133.   Bio-Rad. Droplet Digital PCR Application Guide [Guide]. bio-rad.com 2022 [14.04.22]. Available from: www.bio-rad.com/ddPCRAppGuide.

134.   European Society of Human Reproduction and Embryology; ESHRE. Rules for certification of ESHRE clinical embryologists eshre.eu: ESHRE; 2021 [updated 1.10.2021 cited 07.03.22]. Available from: https://www.eshre.eu/Accreditation-and-Certification/Certification-for-embryologists/Rules-for-Certification-of-ESHRE-embryologists.

135.   Hammond ER, McGillivray BC, Wicker SM, Peek JC, Shelling AN, Stone P, et al. Characterizing nuclear and mitochondrial DNA in spent embryo culture media: genetic contamination identified. Fertility and Sterility. 2017;107(1):220-8.e5.

136.   Carlson BM. Getting Ready for Pregnancy. Human Embryology and Developmental Biology. 6th ed: Elsevier; 2019. p. 1-22.

Appendices

Appendix A: Grading System for Cleavage Stage Embryos

Grade	Rating	Description
1	Good	<10% fragmentation Stage-specific cell size No multinucleation
2	Fair	10-25% fragmentation Stage-specific cell size for majority of cells No evidence of multinucleation
3	Poor	Severe fragmentation (>25%) Cell size not specific Evidence of multinucleation

Appendix B: Grading System for Morula Stage Embryos

Grade	Rating	Description
1	Good	Entered into a fourth round of cleavage. Evidence of compaction that involves virtually all the embryo volume.
2	Fair	Entered into a fourth round of cleavage. Compaction involves the majority of the volume of the embryo.
3	Poor	Disproportionate compaction involving less than half of the embryo, with two or three cells remaining as discrete blastomeres.

Appendix C: Grading System for Blastocyst Stage Embryos

	Grade	Rating	Description
Stages of development	1 2 3 4		Early Blastocyst Expanded Hatched/hatching
ICM	1	Good	Prominent, easily discernible, with many cells being compacted and tightly adhered together
	2	Fair	Easily discernible, with many cells being loosely grouped together
	3	Poor	Difficult to discern, with few cells
TE	1	Good	Many cells forming a cohesive epithelium
	2	Fair	Few cells forming a loose epithelium
	3	Poor	Very few cells

Appendix D: Overview of the Morphological Assessment of the Cultured Embryos and Their Dissociation Status

The embryos were graded according to the Istanbul criteria (Appendix A, B and C). They were given a score based on their developmental stage after thawing until destruction or dissociation. The letter "A"/"B"/"C" represents the grading scheme from appendix A, B or C, used depending on the developmental stage the embryos were in the different grading schemes were used. The days where no entry is given is either associated with the day of thawing and their developmental stage when thawed, or the day where they were either destructed or dissociated.

Embryo Name	Day 3 Grade	Day 4 Grade	Day 5 Grade	Day 6 Grade	Successful dissociation
1	-	-	B, 2	C, Development: 3 ICM: 1 TE: 1	Not attempted
2	-	B, 1	C, Development: 2 ICM: 2 TE: 2	C, Development: 4 ICM: 2 TE: 2	Not attempted
3	-	B, 1	C, Development: 3 ICM: 1 TE: 1	-	Not attempted
4	-	B, 1	C, Development: 1 ICM: 1 TE: 1	C, Development: 3 ICM: 2 TE: 1	Not attempted
5	-	B, 1	C, Development: 3 ICM: 1 TE:1	-	Not attempted
6	A, 1	A, 3	-	-	No
7	-	-	C, Development: 1 ICM: 3 TE: 2	C, Development: 2 ICM: 3 TE: 2	Yes
8	-	-	C, Development: 1 ICM: 3 TE: 1	C, Development: 3 ICM: 1 TE: 1	Yes
9	-	B, 2	B, 3	-	No
10	A, 1	A, 2	A, 3	-	Yes

11	-	B, 2	C, Development: 2 ICM: 2 TE: 1	C, Development: 2 ICM: 2 TE: 1	Yes
12	A, 3	B, 3	-	-	Yes
13	A, 3	A, 3	-	-	Yes
14	-	B, 2	B, 2	C, Development: 1 ICM: 3 TE: 2	No
15	-	-	C, Development: 2 ICM: 1 TE: 1	C, Development: 4 ICM: 1 TE: 1	Yes
16	-	B, 3	B, 3	-	Yes
17	-	-	C, Development: 1 ICM: 2 TE: 2	C, Development: 1 ICM: 3 TE: 3	Yes
18	-	-	C, Development: 2 ICM: 2 TE: 1	C, Development: 2 ICM: 3 TE: 3	Yes
19	-	B, 1	B, 2	C, Development: 1 ICM: 3 TE: 3	Yes
20	-	B, 1	C, Development: 1 ICM: 1 TE: 2	C, Development: 2 ICM: 1 TE: 1	Yes
21	-	B, 1	C, Development: 1 ICM: 2 TE: 2	C, Development: 1 ICM: 3 TE: 3	Yes
22	A, 2	A, 3	-	-	Yes
23	A, 2	A, 3	-	-	No
24	A, 2	A, 3	B, 3	-	Yes
25	A, 3	A, 3	-	-	Yes
26	A, 1	B, 1	C, Development: 1 ICM: 2 TE: 2	C, Development: 1 ICM: 3 TE: 3	Yes
27	A, 1	A, 2	A, 3	-	No

28	A, 1	B, 2	C, Development: 1 ICM: 2 TE: 2	C, Development: 1 ICM: 3 TE: 3	Yes
29	A, 2	B, 1	C, Development: 1 ICM: 3 TE: 2	C, Development: 1 ICM: 3 TE: 3	Yes
30	-	B, 1	B, 3	-	Yes
31	-	B, 1	C, Development: 2 ICM: 1 TE: 1	C, Development: 3 ICM: 1 TE: 1	Yes
32	-	-	C, Development: 1 ICM: 2 TE: 1	C, Development: 1 ICM: 2 TE: 2	Yes
33	-	-	C, Development: 1 ICM: 1 TE: 1	C, Development: 1 ICM: 3 TE: 3	Yes
34	-	B, 1	C, Development: 1 ICM: 2 TE: 1	C, Development: 3 ICM: 1 TE: 1	Yes
35	-	B, 1	B, 3	-	Yes
36	-	-	C, Development: 2 ICM: 2 TE: 1	C, Development: 3 ICM: 2 TE: 1	Yes

Appendix E: Consensus Sequence Alignment

The consensus sequence that was searched against the human genome with Blastn, showing correct alignment in the genome at the right location.

Location	Alignment
chr10: 93094643 - 93094833	AGTGYAGTGGCGTGATCTCGCCCACTACCACACCTGGCTAATTTTTGT ATTTTTAATAGAGATGGGGTTTCACCATCTTGGCCAGGCTGGTCTTGA ACTCCTGACCTCGTGATTCACCTGCCTCGGCCTCCCAAAGTGCTGGAA TTACAGGTGTCAGTCAATGCACCTGGCAAATGGGTACCATTT

Download ⌄   GenBank Graphics   Sort by: E value ⌄

Homo sapiens chromosome 10, GRCh38.p13 Primary Assembly
Sequence ID: NC_000010.11 Length: 133797422 Number of Matches: 4

Range 1: 93094653 to 93094838 GenBank   Graphics   ▼ Next Match ▲ Previous Match

Score	Expect	Identities	Gaps	Strand
334 bits(369)	3e-89	185/186(99%)	0/186(0%)	Plus/Plus

Features: 17349 bp at 5' side: cytochrome p450 26a1 isoform 2
212125 bp at 3' side: myoferlin isoform b

```
Query  1       AGTGYAGTGGCGTGATCTcgcccactaccacacctggctaatttttgtatttttaataga  60
               |||| ||||||||||||||||||||||||||||||||||||||||||||||| ||||||||
Sbjct  93094653 AGTGCAGTGGCGTGATCTCGCCCACTACCACACCTGGCTAATTTTTGTATTTTTAATAGA  93094712

Query  61      gatggggtttcaccatcttggccaggctggtcttgaactcctgacctcgtgattcacctg  120
               ||||||||||||||||||||||||||||||||||||||||||||||||||||||||||||
Sbjct  93094713 GATGGGGTTTCACCATCTTGGCCAGGCTGGTCTTGAACTCCTGACCTCGTGATTCACCTG  93094772

Query  121     cctcggcctcccaaagtgctggaattacaggtgtcagtcaatgcacctggcaaatGGGTA  180
               ||||||||||||||||||||||||||||||||||||||||||||||||||||||||||||
Sbjct  93094773 CCTCGGCCTCCCAAAGTGCTGGAATTACAGGTGTCAGTCAATGCACCTGGCAAATGGGTA  93094832

Query  181     CCATTT  186
               ||||||
Sbjct  93094833 CCATTT  93094838
```